



Arabidopsis thaliana phosphoinositide-specific phospholipase C 2 is required for *Botrytis cinerea* proliferation

Luciana Robuschi^a, Oriana Mariani^b, Enzo A. Perk^a, Ignacio Cerrudo^a, Fernando Villarreal^a, Ana M. Laxalt^{a,*}

^a Instituto de Investigaciones Biológicas, Consejo Nacional de Investigaciones Científicas y Técnicas, Universidad Nacional de Mar del Plata, 7600 Mar del Plata, Argentina

^b Plant Nutrition Laboratory, Institute of Agricultural and Nutritional Sciences, Martin Luther University Halle-Wittenberg, Betty-Heimann-Strasse, 06120 Halle (Saale), Germany.

ARTICLE INFO

Keywords:

Arabidopsis thaliana
Botrytis cinerea
Lipid signaling
phospholipase C
Plant defense
Reactive oxygen species

ABSTRACT

Phospholipase C (PLC) plays a key role in lipid signaling during plant development and stress responses. PLC activation is one of the earliest responses during pathogen perception. *Arabidopsis thaliana* contains seven PLC encoding genes (*AtPLC1* to *AtPLC7*) and two pseudogenes (*AtPLC8* and *AtPLC9*), being *AtPLC2* the most abundant isoform with constitutive expression in all plant organs. PLC has been linked to plant defense signaling, in particular to the production of reactive oxygen species (ROS). Previously, we demonstrated that *AtPLC2* is involved in ROS production via the NADPH oxidase isoforms RBOHD activation during stomata plant immunity. Here we studied the role of *AtPLC2* on plant resistance against the necrotrophic fungus *Botrytis cinerea*, a broad host-range and serious agricultural pathogen. We show that the *AtPLC2*-silenced (*amiR PLC2*) or null mutant (*plc2-1*) plants developed smaller *B. cinerea* lesions. Moreover, *plc2-1* showed less ROS production and an intensified SA-dependent signaling upon infection, indicating that *B. cinerea* uses *AtPLC2*-triggered responses for a successful proliferation. Therefore, *AtPLC2* is a susceptibility (S) gene that facilitates *B. cinerea* infection and proliferation.

1. Introduction

Several lipids and lipid-derived metabolites have been shown to be key players in signal transduction pathways, including the activation of plant defense responses (Laxalt and Munnik, 2002; Munnik and Vermeer, 2010; Hung et al. 2014; Hong et al. 2016). Specially, phosphoinositide-specific phospholipase C (PI-PLC or PLC) activation is one of the earliest host responses triggered by the recognition of several microbe-associated molecular patterns (MAMPs), such as the fungal xylanase, chitosan and N-acetylligosaccharides, as well as the bacterial flagellin-derived peptide flg22 (van der Luit et al. 2000; Laxalt and Munnik, 2002; Laxalt et al. 2007; Raho et al. 2011; Gonorazky et al. 2014; Abd-El-Haliem and Joosten, 2017; D'Ambrosio et al. 2017), or pathogen effector proteins (de Jong et al. 2004; Andersson et al. 2006). PLC catalyzes the hydrolysis of phosphatidylinositol 4-phosphate (PI4P) and phosphatidylinositol 4,5-bisphosphate [PI(4,5)P₂] to produce inositol phosphates (I(1,4)P₂ or I(1,4,5)P₃) and diacylglycerol (DAG) (Meijer and Munnik, 2003). IP₂ and IP₃ diffuse into the cytosol and are

further phosphorylated by inositol polyphosphate kinase (IPK) (Williams et al. 2015) to generate IP₆, which stimulates the release of Ca²⁺ from intracellular reservoirs, affects gene transcription and mRNA export, and is part of the auxin receptor TIR1 (Lemtiri-Chlieh et al. 2000; Meijer and Munnik, 2003; Tan et al. 2007; Li et al. 2015); IP₅, which is part of the jasmonate receptor COI1 (Sheard et al. 2010); and IP₇ and IP₈, which are involved in plant defense (Laha et al. 2015). The other PLC product, DAG, remains in the membrane and is phosphorylated by DAG kinase (DGK) to produce the second messenger phosphatidic acid (PA) (Meijer and Munnik, 2003). PA is considered an important cellular signal transducer, which regulates several protein targets (Arisz et al. 2009; Testerink and Munnik, 2011; Munnik, 2014). PA has been implicated specifically in the modulation of immune signaling components, such as mitogen-activated protein kinases (MAPKs) and phosphoinositide-dependent protein kinase 1 (PDK1) (Farmer and Choi, 1999; Lee et al. 2001; Anthony et al. 2006; Szczegielniak et al. 2006; Galletti et al. 2011; Testerink and Munnik, 2011). In particular, PA binds to the NADPH oxidase isoforms RBOHD and RBOHF to induce ROS

* Corresponding author.

E-mail address: amlaxalt@mdp.edu.ar (A.M. Laxalt).

during abscisic acid (ABA)-mediated stomatal closure (Zhang et al. 2009). Additionally, it has been shown that PLC activity is required for ROS production during MAMP and effector triggered immunity (MTI and ETI, respectively) responses (van der Luit et al. 2000; Laxalt and Munnik, 2002; de Jong et al. 2004; Andersson et al. 2006; Laxalt et al. 2007; Raho et al. 2011; Gonorazky et al. 2014; Abd-El-Haliem and Joosten, 2017; D'Ambrosio et al., 2017). Thus, PLC/DGK pathway is involved in the signaling of plant defense responses (Galletti et al. 2011; Testerink and Munnik, 2011).

The *Arabidopsis thaliana* genome contains seven PLC encoding genes (*AtPLC1* to *AtPLC7*) and two pseudogenes (*AtPLC8* - *AtPLC9*) (Mueller-Roeber and Pical, 2002), being AtPLC2 the most abundant isoform with constitutive expression in all plant organs (Pokotylo et al. 2014). AtPLC2 presents the basic organization of a PLC with two EF-hand motifs, the catalytic domains X and Y, linked by a linker, and the C2 domain (Munnik, 2014). AtPLC2 is rapidly phosphorylated in response to flg22 and oligogalacturonides (Nuhse et al. 2007; Kohorn et al. 2016). We demonstrated that AtPLC2 is involved in MTI during *Pseudomonas syringae* pv. *tomato* (*Pst*) interaction and non-host resistance to the adapted pea powdery mildew *Erysiphe pisi* (D'Ambrosio et al., 2017). AtPLC2 is required for ROS production during flg22 treatments (D'Ambrosio et al., 2017). Consistently, AtPLC2 associates with the NADPH oxidase RBOHD, suggesting its potential regulation by AtPLC2-activity (D'Ambrosio et al., 2017).

Botrytis cinerea is one of the most economically destructive agricultural pathogens. This broad-host range necrotrophic fungus infects almost all vegetables and fruit crops (Dean et al. 2012; Windram et al. 2016). Also represents an important model system to study plant necrotrophs' lifestyle, which thrive at the expense of killing their host (Ghozlan et al. 2020). *B. cinerea* produces ROS, phytotoxins, and cell-wall-degrading enzymes to induce necrosis of plant tissues (van Kan, 2006; van Baarlen et al. 2007), and also triggers programmed cell death pathways in the host, activating ROS production and hypersensitive response (HR), which favors the infection process (van Kan, 2006; Windram et al. 2016; AbuQamar et al. 2017). Besides HR and local cell death, ROS released by the plant in response to pathogen perception, activate the expression of defense-related genes to counteract the pathogen. In *A. thaliana*, transcript levels of flg22 induced receptor-like kinase 1 (FRK1) and the transcription factor WRKY33 are augmented after *B. cinerea* inoculation, which are MAPK- and CDPK-dependent MAMP-activated immune marker genes (Zheng et al. 2006; Boudsocq et al. 2010; Mao et al. 2011; Birkenbihl et al. 2012; Liu et al. 2015). Arabidopsis infection with *B. cinerea* also activates the expression of the salicylic acid (SA)-marker gene, pathogenesis-related protein 1 (PR1) and the jasmonic acid (JA) and ethylene (ET)-marker gene, plant defensin 1.2 (PDF1.2) which encodes a protein with antimicrobial activity (Windram et al. 2012; Ghozlan et al. 2020).

Here we study the role of *A. thaliana* PLC2 on plant resistance against the necrotrophic fungus *B. cinerea*, its relation with ROS production and defense gene expression. Unraveling host responses against *B. cinerea* is a key challenge to understand the pathology of this fungus and may lead to the development of resistant or tolerant crop cultivars.

2. Material and methods

2.1. Plant material and growth conditions

A. thaliana (Columbia-0 ecotype) seeds were produced by growing the plants on soil (soil:vermiculite:perlite, 3:1:1) under 16 h-light/8 h-dark photoperiod at 25 °C. Wild-type and mutant seeds were obtained at the same time and filtered through a 250 µm sieve. Seeds were kept for 48 h at 4 °C before sowing. For fungal infection assays, plants were grown on soil under 8 h-light/16 h-dark cycle at 22 °C. T-DNA insertion line (FLAG_506C04) *plc2-1* (Col-0) reported and kindly provided by Kanehara et al. 2015 was confirmed by PCR and by western blot (Fig. 1). The *amiRPLC2*-silenced line 7 was generated in our laboratory

(D'Ambrosio et al., 2017).

2.2. Leaf-shape analysis

Rosettes from five-week-old plants, grown under short-day condition (22°oC; 8 h-light/16 h-dark), were detached and photographed immediately. Leaves were subsequently removed from the rosette, adhered to white paper using clear adhesive and then scanned (Epson Perfection V600 Photo scanner). Leaf blade-length, -width and -serration level was calculated from leaf silhouettes using ImageJ software as described elsewhere (van Wijk et al. 2018).

2.3. *Botrytis cinerea* inoculum

B. cinerea isolate B05.10 was maintained in cool storage at – 80 °C in 15% glycerol (v/v) until required. For maintenance cultures, *B. cinerea* was grown in 9 cm diameter petri dishes on potato dextrose agar (1.5% agar, 2% potato dehydrated and 2% dextrose) in the dark at 18 °C for 4 d, then the dishes were placed under in black light (380 nm) for 2 d to induce sporulation (Nicot et al. 1996) and grown again in the dark at 18 °C until subculturing. For infection assays, conidia were isolated from a second subculture (Benito et al. 1998; Gonorazky et al. 2016), resuspended in 50 mM sucrose 35 mM phosphate buffer adjusting the final concentration as required (see Section 2.4) and incubated 3 h at room temperature before inoculation.

2.4. Fungal infection assays

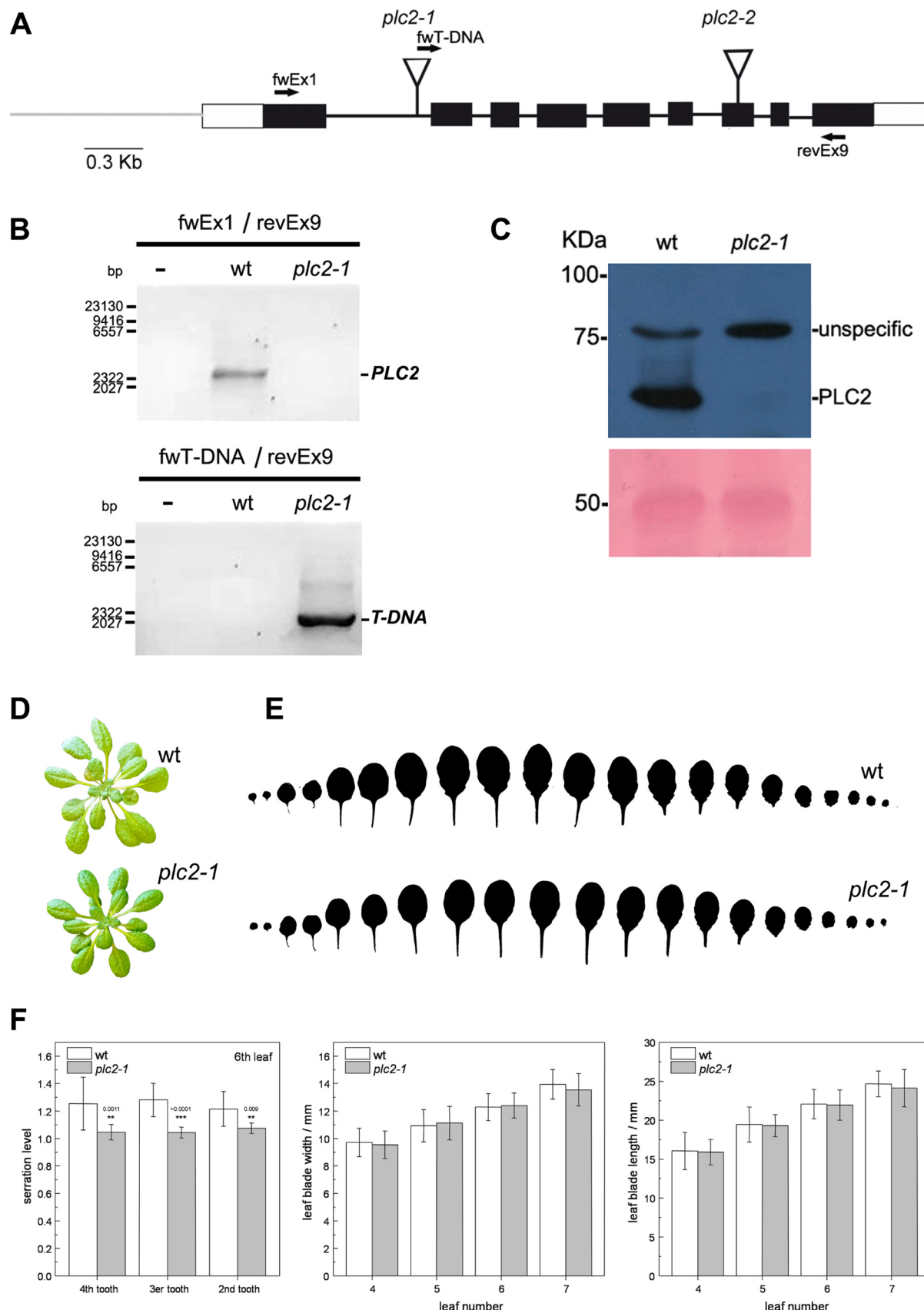
Four to five-week-old *A. thaliana* plants were drop- (for lesion size and H₂O₂ measurements) or spray-inoculated (for gene expression analysis) with *B. cinerea* as described below. For droplet inoculations, 5 µl of *B. cinerea* spore suspension (3 × 10⁵ conidia/ml) were placed on the adaxial surface of four leaves of each plant (4th to 7th leaf, one droplet per leaf) (Muckenschabel et al. 2002). Wild-type and *plc2-1* plants of the same size were selected. Spray inoculations were performed with a 10⁶ conidia/ml suspension. Incubation of inoculated plants was performed at 22 °C under 8 h-light/16 h-dark photoperiod. High humidity was maintained by covering the plants with a clear plastic film (Benito et al. 1998). To quantify *B. cinerea* disease symptoms, necrotic lesion size of drop-inoculated leaves was determined. Inoculated leaves were removed 72 h post inoculation (hpi), scanned and the necrotic area of each leaf was measured from the images acquired with Adobe Photoshop Software v6.0. Results are expressed as necrotic area per plant (sum of the necrotic area of the four infected leaves). Each experiment included 12 plants and three independent experiments.

2.5. Detection of H₂O₂ production in *B. cinerea* infected leaves

For H₂O₂ determinations, drop-inoculated leaves were harvested at 24 hpi and immediately incubated with 15 mg/l 3,3-diaminobenzidine (DAB) in 50 mM sodium acetate pH 5.5 at 25 °C in the dark for 2.5 h (Thordal-Christensen et al. 1997). Leaves were bleached with 96% ethanol. Stain intensity was quantified by using ImageJ Software v 1.53 m. Pictures were transformed to 8-bit and inverted. H₂O₂ production per leaf was expressed as the mean gray value of a fixed area within the infected site minus the mean gray value of the same area of the uninfected background. Two independent experiments were conducted with approximately 30–40 replicates.

2.6. RNA isolation and quantitative RT-qPCR analysis

A. thaliana leaf samples were collected 24 h after mock treatment or fungal infection (spray), frozen in liquid nitrogen and stored at – 80 °C. Each sample consisted of a pool of the treated leaves from three independent plants and each experiment included three samples. After grinding samples in liquid nitrogen, total RNA was isolated using the



(caption on next page)

Fig. 1. AtPLC2 gene structure and insertion mutants. (A) Schematic diagram of AtPLC2. The position of the T-DNA corresponding to the mutants is shown. Exons are indicated as boxes (black: coding region; white: UTR), introns as black lines and promoter region as gray line. Primers used for PCR-based genotyping are indicated. (B) Genotyping of Col-0 wild-type (wt) and *plc2-1* mutant plants analyzed by PCR. (C) AtPLC2 expression in wt and *plc2-1* mutant plants. Protein extraction and Western-Blot analysis was performed as previously described (D'Ambrosio et al., 2017). Top panel: Nitrocellulose membrane incubated with polyclonal anti-PLC2 antibody (1:2,000) and revealed using a secondary anti-rabbit IgG antibody coupled to horseradish peroxidase and ECL detection reagent (BIO-RAD) according to the manufacturer's instructions. Bottom panel: Ponceau S staining (loading control). (D) Rosettes of wt and *plc2-1* mutant plants grown on soil for 5 weeks at 22 °C in 8 h-light/16 h-dark photoperiod. (E) Leaf series of five-week-old wt and *plc2-1* plants shown in Fig. 1D. Leaves were cut and photographed immediately. (F) Quantification of leaf-serration level, -width and -length of leaves from five-week-old wt and *plc2-1* mutant plants. Asterisks denote that means are significantly different from wt plants according to a Dunnett's test.

Trizol method according to the manufacturer's instructions (Invitrogen). The concentration and purity of the isolated RNA was measured with an UV spectrophotometer (NanoDrop™ One, Thermo Scientific). The mean ratio value of A260/280 for all RNA samples was 1.75–2.1 reflecting high purity and protein absence. RNA integrity was verified performing 1% (w/v) agarose gel electrophoresis (data not shown).

One microgram of total RNA from each sample was treated with DNase I RNase-free according to the manufacturer's instruction (Thermo Scientific) and used as template for cDNA synthesis by M-MLV reverse transcriptase (Invitrogen) with oligo(dT) primer in a final volume of 20 µl as previously described (D'Ambrosio et al., 2017). cDNAs were diluted 1:5 with ddH₂O for further analysis.

RT-qPCRs were performed in 96 well plates in 12.5 µl total reaction volume including 2.5 µl of 1:5 dilution of cDNA template, 480 nM primer mix and 6.25 µl of The Fast Universal SYBR Green Master mix from Roche (Mannheim, Germany). Amplified signals were monitored continuously with a Step One Plus Real-Time Thermal Cycler (Applied Biosystem). Thermocycling was performed using the following conditions: 10 min of denaturation and enzyme activation at 95 °C, followed by 40 cycles of: 15 s at 95 °C, 1 min at 60 °C. Melting curve analysis was performed from 60 to 95 °C with 0.3 °C of increment to verify primer specificity. The RT-qPCR assays were performed using three biological and two technical replicates. A no template control (NTC) reaction and a minus RT transcriptase negative control were included in every qPCR run for each primer set. Real time data was analyzed using the StepOne™ Software v2.3 Tool (Applied Biosystem) and LinRegPCR v11.0 (Ruijter et al., 2009). A default threshold of 0.2 was used. The expression levels of the genes of interest were normalized to those of the constitutive actin gene, AtACT2. The nucleotide sequences of the specific primers for qPCR analysis of pathogenesis-related protein 1 (AtPR1), plant defensin 1.2 (AtPDF1.2), WRKY transcription factor 33 (AtWRKY33), flg22 induced receptor-like kinase 1 (AtFRK1) and AtACT2 are listed in Supplementary Table S1. Three biologically independent experiments were performed.

2.7. RT-qPCR statistical analysis

RT-qPCR results were analyzed using general linear mixed models (glmm) with post hoc Dunnett's method comparisons. We have developed one general linear mixed-effects model for each gene, using the lme or glmer function from the nlme library in R Software v3.1 (R Foundation for Statistical Computing). Fixed effects were Treatment and Line, response variable was relative gene expression and replicate was used as random effect. Error distribution employed were Gaussian or Gamma, and in certain cases logarithmic transformation on response variable was applied.

2.8. Characterization of the linker region in AtPLC2 and SIPLC2 homologues

The training dataset was obtained from the phylogeny presented in Perk et al. (2023). In addition, we generated a PLC target dataset using complete proteomes from additional 25 lamiids and 40 malvids species, including 14 Solanaceae and 21 Brassicaceae, respectively (Supplementary Table S2). The sequence mining for the target was performed with hmmsearch (HMMER3) (Eddy, 2011) using a plant PLC specific

hmmer profile. The sequences were then classified into the training dataset using HMMERCTTER (Pagnucco et al. 2018). From the resulting dataset, we focused on those sequences classified in the clade from the training containing AtPLC2 and SIPLC2 which also includes AtPLC7 and SIPLC3 (Supplementary Table S3 and Supplementary File S1), and were used to reconstruct a dedicated phylogeny. For this, sequences were aligned using MAFFT G-INS-i (Katoh and Standley, 2013), pruned with BMGE (Criscuolo and Gribaldo, 2010) with gap 0.5 and entropy 0.8, and maximum likelihood tree generated with PhyML (Guindon et al. 2010), using WAG model. The intrinsically disordered regions (IDRs) were predicted using MobiDB, which integrates data from 9 IDR prediction tools into a consensus prediction (Piovesan et al. 2023). This information was compared to the structural AlphaFold2 (Jumper et al. 2021) model of AtPLC2 available at Uniprot (PLCD2_ARATH, Q39033) to confirm the localization of the X-Y linker. The linker region for each clade was extracted from the multiple sequence alignment, and used to generate the sequence logos with Weblogo 3 (Crooks et al. 2004).

3. Results

3.1. AtPLC2-silenced plants and *plc2-1* mutant plants are more resistant to the necrotrophic fungus *Botrytis cinerea*

Previously, two independent T-DNA insertion AtPLC2 mutant lines were studied, one in Wassilewskija (Ws; *plc2-1*) and the other in Columbia-0 (Col-0; *plc2-2*) ecotype (Fig. 1A). Both *plc2-2* and *plc2-1* knock-out mutants were lethal, showing that AtPLC2 was necessary for gametophyte and embryo development (Li et al. 2015; Di Fino et al. 2017; Chen et al. 2019). To overcome gametophyte defects, we performed AtPLC2 silencing in Col-0 background by expressing artificial microRNAs in the sporophyte and obtained viable plants, with lower AtPLC2 expression in leaves (D'Ambrosio et al., 2017). At the same time Kanehara et al. (2015) reported that *plc2-1* homozygous knock-out plants were phenotypically normal in Ws background as well as in Col-0 background (*plc2-1* mutant in Ws ecotype was backcrossed with wild-type Col-0 six times to replace the ecotypical background) (Kanehara et al. 2015). Thus, in order to study the role of AtPLC2 during *Botrytis* infections we requested the *plc2-1* seeds backcrossed in Col-0. First, we checked the interruption of the AtPLC2 gene using specific primers and the presence of the T-DNA insertion within the first intron of the gene (Fig. 1B). In addition, *plc2-1* plants did not show AtPLC2 protein using specific AtPLC2 antibodies (Fig. 1C). *plc2-1* plants present a slightly different morphology, with more rounder leaves than wild-type plants, due to shorter leaf serration level (Fig. 1D to F). No significant differences were seen in the leaf blade width and length of five-week-old wild-type and *plc2-1* plants (Fig. 1F). Plants of this age were used for the following experiments.

In this context, in order to investigate whether AtPLC2 is involved in *A. thaliana* defense response against the necrotrophic fungus *B. cinerea*, wild-type, AtPLC2-silenced (*amiR PLC2*) (D'Ambrosio et al., 2017) and *plc2-1* knock-out (Kanehara et al. 2015) plants in Col-0 background were inoculated with *B. cinerea* spore suspension and leaf disease symptoms were evaluated by determining the necrotic area 72 h after fungal infection (hpi) (Fig. 2). The results show that *amiR PLC2* and *plc2-1* leaves have smaller necrotic lesions (nearly 30% and 60%, respectively) than those formed in wild-type leaves, indicating that

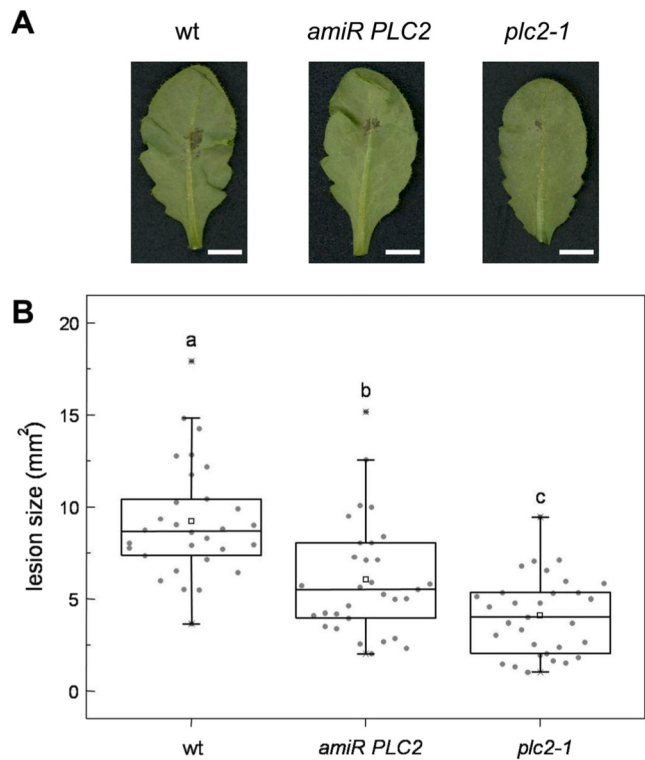


Fig. 2. AtPLC2 is required for *A. thaliana* susceptibility to *B. cinerea*. Four to five-week-old wild-type (wt), *PLC2*-silenced (*amiR PLC2*) or *plc2-1* mutant *A. thaliana* plants were drop-inoculated in the 4 to 7th leaf with *B. cinerea* isolate B05.10 spore suspension (3×10^5 conidia/ml). (A) Representative pictures of infected leaves 72hpi (Scale bars:0.5 cm). (B) Disease symptoms, expressed as lesion size per plant (sum of the necrotic area of the four inoculated leaves) were measured at 72hpi with Adobe Photoshop v6.0. Error bars represent standard errors of three independent experiments. Different letters denote means significantly different according to a Dunnett's test ($P < 0.05$).

PLC2-silenced and *plc2-1* knock-out plants are more resistant to *B. cinerea* (Fig. 2) evidencing that AtPLC2 participates in plant susceptibility to *B. cinerea*. As expected, *AtPLC2*-silenced line presents an intermediate phenotype between knock-out *plc2-1* and wild-type plants, therefore we proceeded our studies with the knock-out mutants.

3.2. AtPLC2 is involved in the *B. cinerea*-induced ROS burst

Previously, we demonstrated that AtPLC2 participates in the regulation of the NADPH oxidase RBOHD during plant defense responses upon flagellin treatments and *Pseudomonas* infections (D'Ambrosio et al., 2017). Thus, we further investigate if AtPLC2 is also involved in ROS production during *B. cinerea* infection. We evaluated H₂O₂ levels, a major component of ROS, in *B. cinerea* drop-inoculated leaves by the DAB-stain method (Thordal-Christensen et al., 1997). Quantification results and representative pictures are shown in Fig. 3. On infected wild-type leaves, a brown DAB staining indicative of H₂O₂ accumulation was clearly visible 24hpi, confirming that *B. cinerea* induces a ROS burst in *A. thaliana* plants (Fig. 3). When compared with wild-type plants, *plc2-1* mutant plants exhibited a significant reduction in ROS levels (about 40%) in response to *B. cinerea* (Fig. 3B), indicating that AtPLC2 is required for the full ROS burst after *B. cinerea* recognition in *A. thaliana* leaves. No stains were visualized in mock treatments of wild-type or *plc2-1* plants (Fig. S1).

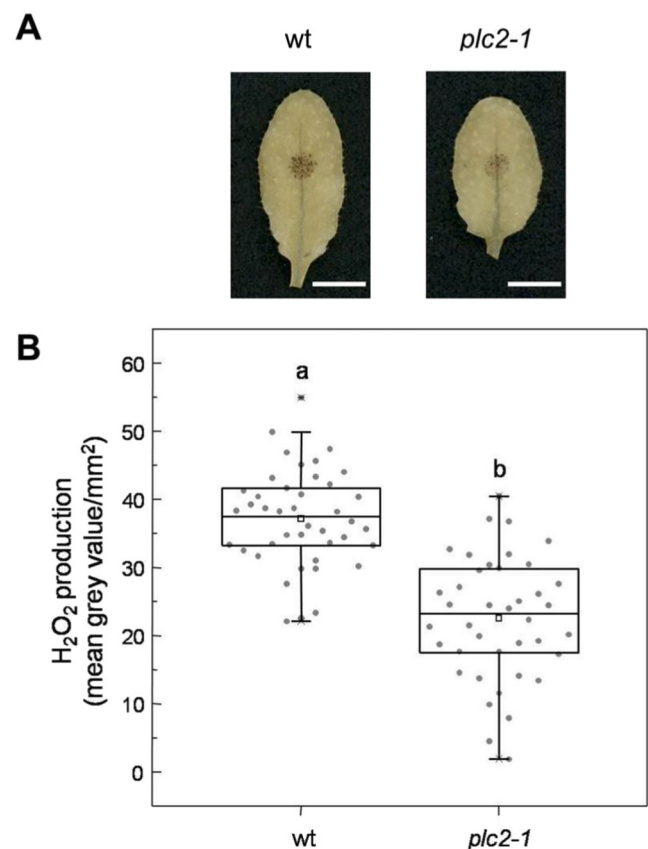


Fig. 3. AtPLC2 is required for H₂O₂ production in response to *B. cinerea* infection. Four to five-week-old wild-type (wt) or *plc2-1* mutant *A. thaliana* plants were drop-inoculated in the 4 to 7th leaf with *B. cinerea* spore suspension (3×10^5 conidia/ml). Leaves were harvested 24hpi and H₂O₂ production was detected by DAB staining immediately after harvesting. (A) DAB-stained tissue was macroscopically observed. Pictures from representative leaves 24hpi are shown (Scale bars: 0.5 cm) (B) Quantification of DAB intensity at the stained area was expressed as mean gray value/ mm^2 . Error bars represent standard errors of two independent experiments, with approximately 30–40 drops per experiment. Different letters denote means significantly different according to Dunnett's test ($P < 0.05$).

3.3. AtPLC2 mediated host responses against *B. cinerea* are SA- but not JA/ET-dependent

As mentioned, downstream of ROS other responses such as the expression of defense-related genes are triggered (Levine et al. 1994). To address if AtPLC2 is involved in these responses we analyzed by qPCR the *B. cinerea*-induced expression levels of the defense-related gene markers *AtFRK1*, *AtPR1*, *AtPDF1.2* and *AtWRK33* in *plc2-1* plants after 24 h of fungal infection (Fig. 4). As expected, in wild-type plants the transcript levels of the defense-related gene markers are induced in response to *B. cinerea* infection as previously reported (Fig. 4) (Galletti et al. 2011; Birkenbihl et al. 2012). Interestingly, qPCR analysis revealed that the relative expression of *AtFRK1* 24hpi was significantly higher in *plc2-1* compared to wild-type plants (Fig. 4), consistent with the observed resistance phenotype, indicating that AtPLC2 negatively regulates *AtFRK1* expression in *A. thaliana* infected by *B. cinerea*. The basal *AtFRK1* expression level in *plc2-1* was higher than the basal level in wild-type plants, but independently of that, in *B. cinerea* infected tissue was notoriously higher (Fig. 4 and Fig. S2). Similarly, the expression of the SA-regulated gene *AtPR1* was induced 10 times more in *plc2-1* leaves compared to wild-type plants at 24 hpi. These results suggest that AtPLC2 acts as a negative regulator of the SA-dependent response, indicating that *plc2-1* resistance to *B. cinerea* is at least in part

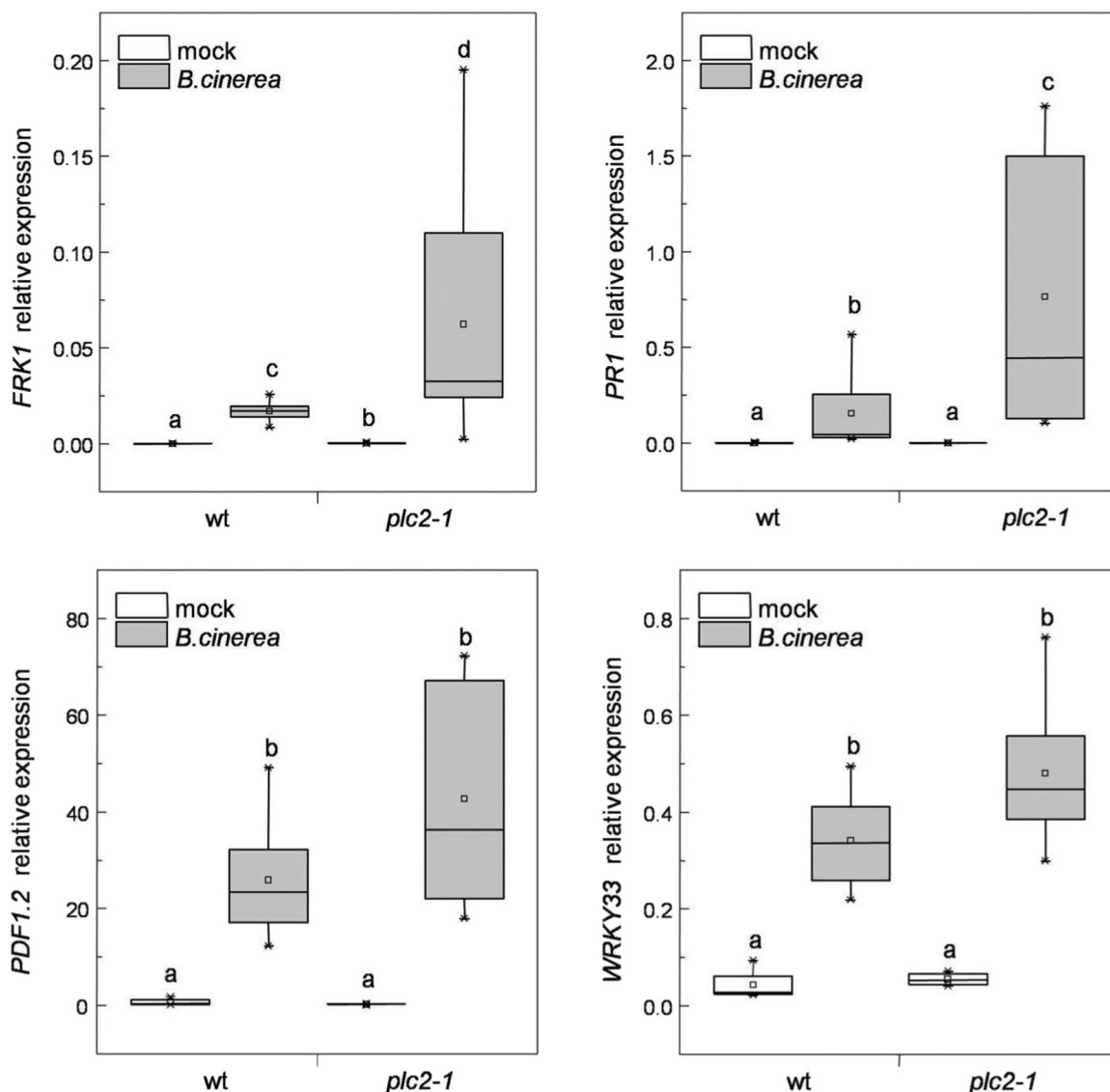


Fig. 4. Transcript levels of plant-defense gene markers in *plc2-1* mutant plants in response to *B. cinerea* infection. Four to five-week-old wild-type (wt) or *plc2-1* mutant *A. thaliana* plants were spray-inoculated with *B. cinerea* spore suspension (10^6 conidia/ml). Leaves were harvested 24hpi. Total RNA was isolated and transcript levels of flagellin-induced receptor-like *FRK1*, SA-defense gene marker *PR1*, JA/ET-defense gene marker *PDF1.2* and transcription factor *WRKY33* were determined by RT-qPCR. Transcript levels were normalized to *AtACT2*. Error bars represent standard errors of three independent experiments, with three biological replicates per experiment. Different letters denote medians significantly different according to a Dunnett's test ($P < 0.05$).

SA-dependent. In contrast, the JA/ET-related immune marker *AtPDF1.2* and the transcription factor *AtWRKY33* did not differ between *plc2-1* and wild-type infected plants.

In tomato, we have previously demonstrated that silencing and knocking-out *SlPLC2* resulted in decreased ROS production and reduced *B. cinerea* infection (Gonorazky et al. 2016; Perk et al. 2023), as reported here in Arabidopsis. However, in tomato knock-down and knock-out of *SlPLC2* resulted in diminished transcript levels of the SA-related defense gene *SlPR1*, while transcripts of the JA-related defense genes Proteinase Inhibitor I and II (*SlPI-I* and *SlPI-II*) augmented in response to *B. cinerea* (Gonorazky et al. 2016; Perk et al. 2023). The above-mentioned results are in contrast with the findings reported here in Arabidopsis, suggesting that possibly AtPLC2 and SlPLC2 have different and specific defense pathways against *B. cinerea* in each species.

In order to unravel plausible regulation differences, we compare the sequence of AtPLC2 with enzymes that belong to the same clade as AtPLC7, SlPLC2 and SlPLC3 (Perk et al. 2023). It has been reported that intrinsically disordered regions (IDRs) are targets for post-translational

modifications such as phosphorylation (Iakoucheva et al. 2004; Bah and Forman-Kay, 2016). AtPLC2 has a disordered region between the catalytic domains called X-Y linker (Fig. 5A). In particular, the serine that is phosphorylated in AtPLC2 (S280) upon flg22 and oligogalacturonic acid (Nuhse et al. 2007; Kohorn et al. 2016) is located in this region (Fig. 5A, highlighted with a yellow arrow). In addition, AtPLC7, SlPLC2 and SlPLC3 also possess a disordered X-Y linker (Fig. 5A), although to the best of our knowledge, no concrete evidence of activity modulation mediated by phosphorylation for these enzymes has been reported. To further analyze the linker region of these PLCs, we increased the amount of information by adding more homologous malvids and lamiids PLC sequences to the analysis. Using the PLC phylogeny from Perk et al. (2023) as training, we classified sequences from additional 65 malvids and lamiids species (Table S2). As a result, the clade 2 from Perk et al. (2023), which originally includes 17 sequences, incorporated a total of 54 malvids sequences and 25 lamiids sequences (96.2% of them from either Brassicaceae or Solanaceae). This results in a PLC classified dataset of 96 sequences. A phylogenetic tree derived from the classified

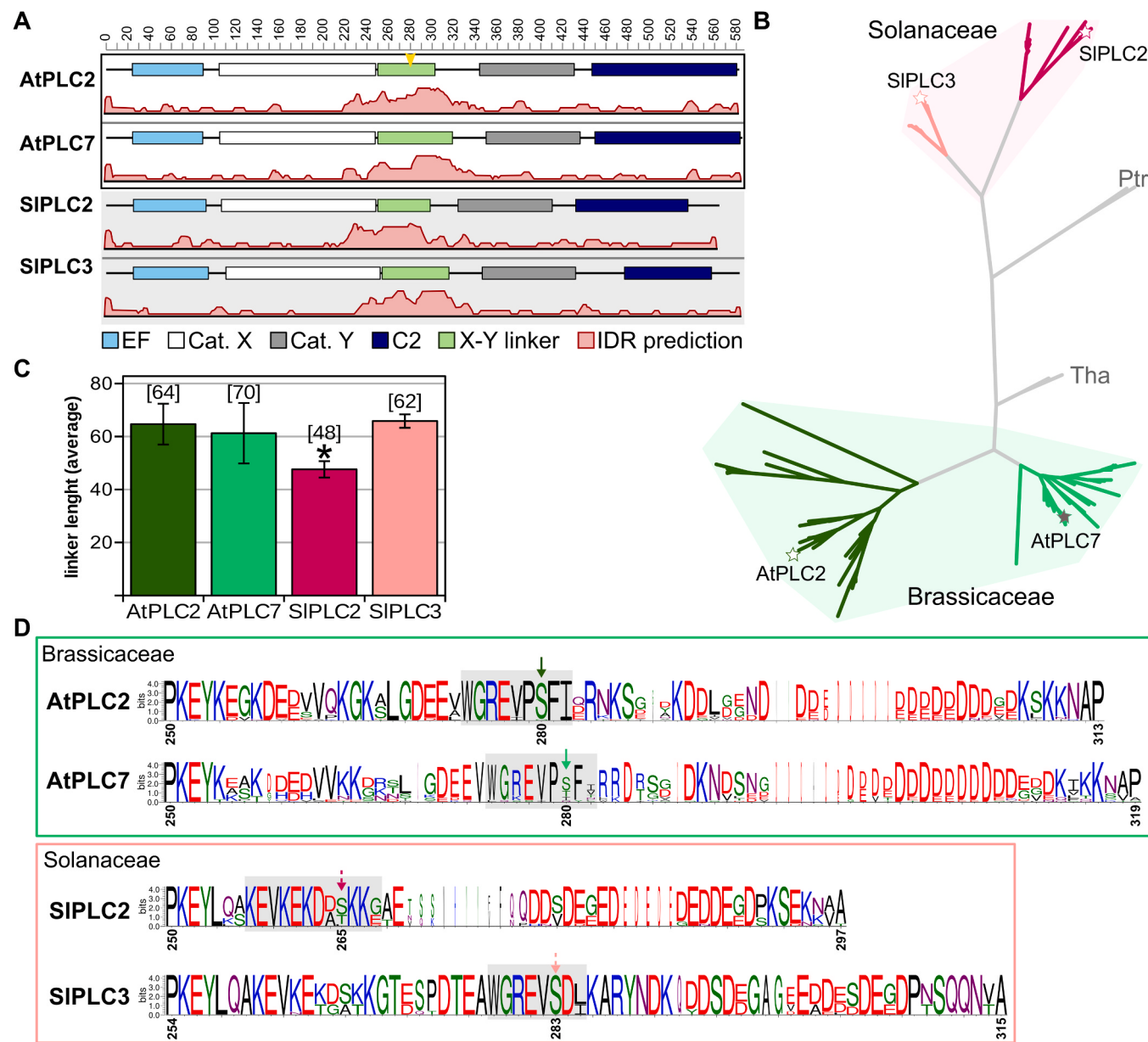


Fig. 5. A comparative analysis of the X-Y linker of AtPLC2 and related protein clades: disorder region analysis and amino acid conservation around the phosphorylated Serine 280. (A) The X-Y linker residues in AtPLC2, AtPLC7, SIPLC2 and SIPLC3 are predicted as IDR, represented in the y-axis shown in the respective plots (consensus prediction from MobiDB). For each protein, the main domains (EF hand, catalytic X and Y, and C2) and the X-Y linker are indicated. Yellow arrowhead: phosphorylated Ser280. (B) Maximum likelihood phylogeny with classified dataset. The main subclades are colored (green shades, Brassicaceae; pink shades, Solanaceae). The sequences from other families are shown in gray (Ptr = *Populus trichocarpa*, Sin = *Sesamum indicum*, Tha = *Tarenaya hassleriana*, Vvi = *Vitis vinifera*). Stars indicate the reference sequence for each subclade (AtPLC2, AtPLC7, SIPLC2 or SIPLC3). (C) The linker length for all sequences in each subclade is shown as average \pm s.d. The number in square brackets corresponds to the linker length in the reference sequence for each clade (AtPLC2, AtPLC7, SIPLC2 and SIPLC3). Star denotes statistical difference (ANOVA and Tukey post-test, $P < 0.001$). (D) The sequence logo of the linker in each subclade is shown. The arrows indicate the position of potential phosphorylatable residue (Ser280 in AtPLC2). The grey box highlights the motif surrounding the putative phosphorylatable residue. Numbers in the sequence logos indicate the beginning and end of the linker, and the position of the putative phosphorylatable position, corresponding to the reference in each clade. X-axis: column information content in bits. Position width represents gap content (highly gapped regions are thinner).

PLC dataset shows the sequences are subdivided in four major subclades, two with sequences only from Brassicaceae (with AtPLC2 and AtPLC7) and other two with sequences from Solanaceae (with SIPLC2 and SIPLC3) (Fig. 5B). The representation of most species in each subclade indicates a degree of functional conservation, with the exception of the clade where SIPLC2 belongs, for which several Solanaceae species do not have an homologue (Table S3). Interestingly, the X-Y linker region of the sequences in subclade SIPLC2 is remarkably dissimilar to the homologous region in other subclades. First, the linker in subclade SIPLC2 is the shortest in average (Fig. 5C). In addition, the conservation of

phosphorylatable (or putative phosphorylatable) residues in the linkers from the subclades is very high in subclades AtPLC2 (which corresponds to Ser280) and SIPLC3, and partially conserved in subclades AtPLC7 and SIPLC2 (Fig. 5D). However, the motif surrounding the Ser residue is conserved in the SIPLC2 clade, but very dissimilar compared to the rest of the clades. In this sense, the motif in SIPLC2 contains several basic and acid residues (KEVKEKD[AD][ST]KK), whereas a motif WGREV[-P][ST][FD][LI] is mainly conserved in the remaining clades. Since the X-Y linker, as other IDRs, are involved in interaction with other proteins (e.g., kinases), these results suggest that SIPLC2 may be interacting with,

and responding to, different cognates compared to the rest of the members of the clade (i.e. AtPLC2). In addition, the transcript levels of *SlPLC2* are low under non-infected conditions and induced upon *B. cinerea* infections (Perk et al. 2023), whereas *AtPLC2* is highly and constitutively expressed (Fig. S3) indicating that the promoter regions are different between the two genes.

Altogether, the results suggest that *AtPLC2* and *SlPLC2* may have different post-translational regulation and in consequence different activation pathways that overall will modulate dissimilar responses in each species.

4. Discussion

Lipid signaling is essential for the activation of defense responses in plants (Laxalt and Munnik, 2002; Munnik and Vermeer, 2010; Hung et al. 2014; Hong et al. 2016). In particular, activation of PLC is one of the earliest plant responses after pathogen or MAMP recognition (van der Luit et al. 2000; Laxalt and Munnik, 2002; Raho et al. 2011; Gonozak et al. 2014; Abd-El-Haliem and Joosten, 2017; D'Ambrosio et al. 2017). In this study, we showed that *AtPLC2* null mutant, *plc2-1*, is less susceptible to *B. cinerea* fungal infection, with a reduction in the necrotic lesion size, less H₂O₂ production and an exacerbated induction of the transcript levels of the defense-related genes *AtFRK1* and *AtPR1*; thus, providing evidence that *AtPLC2* is a susceptibility (S) gene that facilitates *B. cinerea* infection and proliferation.

A common early response of plant cells to pathogen attack and elicitor treatment is the oxidative burst (Lamb and Dixon, 1997). However, necrotrophic pathogens benefit from ROS produced by the host to promote cell death, thereby contributing to disease progression (van Kan, 2006; Torres, 2010; Morales et al. 2016). Aggressiveness of *B. cinerea* isolates correlates with the amount of H₂O₂ and OH⁻ radicals present in the leaf tissue during infection (Ghozlan et al. 2020). Our results showed that knocking-out and knocking-down *AtPLC2* resulted in a significant reduction of the lesion size produced by *B. cinerea* in *A. thaliana* leaves. In addition, infected *plc2-1* showed less H₂O₂ production than infected wild-type plants. These results suggest that *AtPLC2* is mediating the oxidative burst induced by *B. cinerea* and is required for the plant's susceptibility to the fungus. The decreased ROS levels observed in *plc2-1* mutants, along with their more resistant phenotype, suggest that ROS generated by the plant could either contribute to the expansion of necrotic lesions caused by *B. cinerea* or negatively affect disease resistance to the fungus. RBOHD is responsible for most of the ROS produced during Arabidopsis defense responses (Torres et al. 2002; Torres, 2010; Marino et al. 2012) and, in particular, RBOHD is the most up-regulated NADPH oxidase during *B. cinerea* infection (Govrin and Levine, 2000; Morales et al. 2016). PLC inhibition reduced NADPH oxidase-dependent ROS production during elicitor treatments (de Jong et al. 2004). It has been demonstrated that phosphatidic acid (PA) and Ca⁺² positively regulates NADPH oxidase activity with the consequent increase of H₂O₂ (Zhang et al. 2009). In addition, we have previously reported that *AtPLC2* interacts constitutively with RBOHD and participates in the regulation of RBOHD upon flg22 treatment and Pseudomonas infection (D'Ambrosio et al., 2017). Therefore, it could be speculated that the ROS burst mediated by *AtPLC2* could be through the activation of RBOHD. However, *rbohD* knock out mutant was shown to be as susceptible to *B. cinerea* as wild-type plants (Galletti et al. 2008; Birkenbihl et al. 2012). Furthermore, the activation of RBOHF might be associated with the necrosis process (Morales et al. 2016), but there is currently no evidence regarding its implication in the response to *B. cinerea* or its interaction with any PLC. Further research is required to elucidate the specific role of *AtPLC2* in regulating ROS levels during Botrytis infections.

PLC-derived second messengers, generated upon PLC activation, play a crucial role in various downstream responses. These include the activation of calcium-dependent protein kinases (CDPKs) and mitogen-activated protein kinases (MAPKs), as well as the regulation of gene

expression (Farmer and Choi, 1999; Lee et al. 2001; Anthony et al. 2006; Szczegielniak et al., 2006; Zhang et al. 2009; Galletti et al. 2011; Testerink and Munnik, 2011). PA, a product of PLC activity, serves as a versatile regulator of protein function and intracellular localization through its binding interactions (Yao and Xue, 2018). For instance, PA has been shown to inhibit the activity of AtCTR1, a negative regulator of ET signaling (Testerink et al. 2007). Upon *B. cinerea* infection, the transcript levels of *AtWRKY33*, a key transcriptional regulator of hormonal and metabolic responses towards *B. cinerea* (Zheng et al. 2006; Birkenbihl et al. 2012; Liu et al. 2015), revealed no differences between *plc2-1* and wild-type plants. Similarly, *B. cinerea*-induced expression of the ET/JA-related gene *AtPDF1.2* was similar in both mutant and wild-type plants, indicating that *AtPLC2* is not involved in the regulation of these genes during *B. cinerea* infection. However, an unexpected up-regulation of *AtFRK1*, a MAPK-dependent immune gene, was observed in *plc2-1* plants in response to *B. cinerea*, indicating that *AtPLC2* negatively regulates MAPK-dependent signaling during *B. cinerea* infection. Further investigation is needed to understand the potential impairment of MAPK signaling in *plc2-1*. Moreover, *plc2-1* plants exhibited an exacerbated up-regulation of SA-induced gene *AtPR1*, indicating that *AtPLC2* also negatively regulates the SA-dependent response against the fungus. Interestingly, in response to flg22, PLC2-silenced plants showed no significant differences in the expression levels of *AtWRKY33* and *AtFRK1* compared to wild-type plants (D'Ambrosio et al., 2017), suggesting that the role of *AtPLC2* and the downstream signaling cascade that is activated is specific and pathogen-dependent. In summary, these results indicate that MAPK- and SA-dependent, but not JA/ET-dependent defense responses are inhibited by *AtPLC2* during *B. cinerea* infection in *A. thaliana*.

SA has been traditionally associated with defense against biotrophic pathogens (those that parasitize a living host), whereas JA and ET signaling appear to be more important against necrotrophic pathogens (Thomma et al. 1999). However, there is increasing evidence that SA does appear to have a role in local immunity against *B. cinerea* (Ferrari et al. 2003; Windram et al. 2016; AbuQamar et al. 2017). The exacerbated SA-response induced by *B. cinerea* in the *plc2-1* line could be, along with the decreased ROS production, an additional cause of the increased resistance observed in this mutant. Furthermore, SA has been reported to antagonize multiple actions mediated by ABA (De Torres Zabala et al. 2009; Moeder et al. 2010), which is a key virulence component of *B. cinerea* (Audenaert, 2002; Cao et al. 2011). *B. cinerea* itself produces ABA and induces water-soaking lesions during the early infection process (Audenaert, 2002; Cao et al. 2011). Besides, ABA negatively regulates plant resistance to certain necrotrophic fungi, since ABA-deficient (i.e. aba2) and ABA signaling mutants (i.e. abi1) showed increased resistance to these pathogens compared to wild-type plants (Audenaert, 2002; AbuQamar et al. 2006; Hernández-Blanco et al. 2007). Interestingly, ABA-deficient tomato mutants present elevated SA levels and enhanced resistance to *B. cinerea* (Audenaert, 2002), a similar phenotype to that observed in the PLC2-deficient Arabidopsis plants. Whether *AtPLC2* is involved in any aspect of ABA signaling in the host defense response triggered by *B. cinerea* remains to be determined.

Pathogen-induced PA can be generated either through PLC/DKG or PLD enzymatic pathways. Recent studies have implicated Arabidopsis PLD δ in the plant response to the fungal MAMP chitin (Xing et al. 2019), indicating the presence of non-redundant PA signaling pathways in plant immunity. Moreover, Zhao et al. (2013) showed that genetic inactivation of PLD $\beta 1$ resulted in enhanced susceptibility to *B. cinerea* infection but increased resistance to *P. syringae* tomato pv DC3000, accompanied by higher levels of ROS and SA (Zhao et al. 2013). On the other hand, genetic inactivation of PLD $\gamma 1$ led to increased resistance to both *P. syringae* tomato pv DC3000 and *B. cinerea* infections, along with elevated ROS levels (Schlöffel et al. 2020). However, alterations in PA levels are unlikely to be the cause of this increased resistance, as they appear to be unaffected in *pld γ 1* mutant plants. Interestingly, PLD $\gamma 1$ has been found to interact with the BAK1-interacting LRR receptor-like

kinases (RLKs) BIR2 and BIR3, revealing a novel function for phospholipases in plant immunity (Schlöffel et al. 2020). Among the DGK-deficient lines tested, DGK5 has been identified as the major isoform responsible for the production of flg22-induced PA. The *dkg5.1* mutant exhibited reduced levels of both PA and ROS after flg22 treatment compared to wild-type seedlings (Kalachova et al. 2022). These findings highlight the complexity of phospholipase-mediated signaling in plant immunity, with different enzymes and pathways playing distinct roles in modulating the plant's defense response to various pathogens and elicitors. Further research is needed to fully understand the specific mechanisms and interactions involved in these processes.

The catalytic function of the phospholipases resides on the X and Y domains, which together form a three-dimensional hollow barrel-shaped structure (TIM-barrel) that holds the active sites inside (Essen et al. 1996; Hunt et al. 2004; Katan and Cockcroft, 2020). The X-Y linker that connects the two domains is a region with a high level of structural disorder, which in turn exhibits little conservation both in length and at the sequence level across the different classes of PLCs. These intrinsically disordered regions (IDRs) are portions of the protein that lack a classic secondary structure (alpha-helix or beta sheet) and have greater mobility. In many cases it has been seen that these disordered regions are targets for post-translational modifications such as phosphorylation, which induce a variety of structural changes in them, stabilizing certain conformations over others (Iakoucheva et al. 2004; Bah and Forman-Kay, 2016). This is the case of AtPLC2, which has the phosphorylatable Ser in the disordered region of the X-Y linker (S280), that could affect the enzymatic activity by changing the three dimensional position of the X and Y catalytic domain. Phylogeny analysis groups AtPLC2 within the same clade as AtPLC7, SIPLC2 and SIPLC3 (Perk et al. 2023). However, we found that the sequences are separated taxonomically in one Brassicaceae and one Solanaceae clade, indicating taxonomically rather than functional grouping. A deeper comparative analysis of the clade revealed i) a significantly shorter X-Y linker in SIPLC2 (48 pb), compared with the rest of the PLCs analyzed (62–70 pb), ii) the conservation of the (putative) phosphorylatable Ser appears higher in subclades AtPLC2 and SIPLC3, and less conserved in subclades AtPLC7 and SIPLC2 and iii) the motif of the adjacent region to the phosphorylation site is similar in AtPLC2, AtPLC7 y SIPLC3, but conspicuously different in SIPLC2.

An aspect that may be related to the phylogenetic relationships of the tree has to do with the regulatory mechanisms of the PLCs. The conserved S280 and its adjacent region in AtPLC2 and AtPLC7 could be an activation/modulation mechanism specific to these two sequences. However, up to date there are no reports on AtPLC7 participation on biotic stress. Previously, we reported that *SIPLC2* is also a susceptibility gene in the response to *B. cinerea* since silencing and knocking-out *SIPLC2* resulted in decreased ROS production and reduced fungal infection (Gonorazky et al. 2016; Perk et al. 2023). Despite the similarity in phenotypes, the differences in the sequence of the X-Y linker between AtPLC2 and SIPLC2 suggest different post-translational regulation mechanisms. In addition, the transcript levels of both genes are differentially regulated indicating that the promoter regions are different between the two genes (Perk et al., 2023; Fig S3). As AtPLC2 in Arabidopsis, SIPLC3 is the most abundant PLC isoform in tomato (Gonorazky et al. 2016; Perk et al. 2023). The similarities in the length, the conservation around the putative phosphorylatable Serine indicate that the SIPLC3, and not SIPLC2 might be regulated in a similar way as AtPLC2. However, there is no evidence until today that indicates that SIPLC3 or any other SIPLC get phosphorylated upon stress or during development. To further investigate this, we are currently editing SIPLC3 to generate knock-out tomato plants and evaluate its role in plant defense, allowing future comparison with AtPLC2.

In conclusion, our study demonstrates the essential role of AtPLC2 as a susceptibility gene in the context of *B. cinerea* infection. The presence of AtPLC2 is required for optimum ROS production during the infection, and the absence of AtPLC2 leads to an up-regulation of the MAPK- and

SA-dependent gene expression. The contrasting resistance phenotype observed between *plc2-1* and wild-type plants against *B. cinerea* presents an opportunity to further investigate the regulatory mechanisms of AtPLC2 in the Arabidopsis/Botrytis system. The findings from this research contribute to our understanding of lipid signaling in plant defense mechanisms, providing valuable insights into how plants respond to pathogen attacks. Moreover, the identification of AtPLC2 as a key player in this signaling network opens up possibilities for the improvement of crop resistance against *B. cinerea* by targeting related genes. Ongoing and future studies focusing on the molecular basis underlying lipid signaling will enhance our knowledge on how the AtPLC2-signaling network operates in the plant defense response, bringing us closer to developing effective strategies for crop protection.

Funding

This work was supported by UNMdP, Consejo Nacional de Investigaciones Científicas y Técnicas (CONICET) and Agencia Nacional de Promoción Científica y Tecnológica (ANPCyT; PICT 2021, PICT 2019).

CRediT authorship contribution statement

Perk Enzo A: Data curation, Methodology. **Robuschi Luciana:** Formal analysis, Investigation, Methodology, Writing – original draft. **Mariani Oriana:** Formal analysis, Investigation, Methodology, Writing – original draft, Writing – review & editing. **Laxalt Ana M.:** Conceptualization, Funding acquisition, Project administration, Resources, Supervision, Writing – review & editing. **Cerrudo Ignacio:** Methodology. **Vallareal Fernando:** Formal analysis, Investigation, Methodology, Writing – original draft.

Declaration of Competing Interest

The authors declare that they have no known competing financial interests or personal relationships that could have appeared to influence the work reported in this paper.

Data Availability

No data was used for the research described in the article.

Acknowledgments

We thank Sergio Batista for greenhouse assistance.

Appendix A. Supporting information

Supplementary data associated with this article can be found in the online version at doi:[10.1016/j.plantsci.2023.111971](https://doi.org/10.1016/j.plantsci.2023.111971).

References

- A.M. Abd-El-Haliem, M.H. Joosten, Plant phosphatidylinositol-specific phospholipase C at the center of plant innate immunity, *J. Integr. Plant Biol.* 59 (3) (2017) 164–179.
- S. AbuQamar, X. Chen, R. Dhawan, B. Bluhm, J. Salmeron, S. Lam, R.A. Dietrich, T. Mengiste, Expression profiling and mutant analysis reveals complex regulatory networks involved in Arabidopsis response to Botrytis infection, *Plant J.* 48 (1) (2006) 28–44, <https://doi.org/10.1111/j.1365-313X.2006.02849.x>.
- S. AbuQamar, K. Moustafa, L.-S. Tran, Mechanisms and strategies of plant defense against Botrytis cinerea, *Crit. Rev. Biotechnol.* 37 (2017) 262–274, <https://doi.org/10.1080/07388551.2016.1271767>.
- M.X. Andersson, O. Kourtchenko, J.L. Dangl, D. Mackey, M. Ellerström, Phospholipase-dependent signalling during the AvrRpm1- and AvrRp1-induced disease resistance responses in Arabidopsis thaliana, *Plant J.* 47 (6) (2006) 947–959, <https://doi.org/10.1111/j.1365-313X.2006.02844.x>.
- R.G. Anthony, S. Khan, J. Costa, M.S. Pais, L. Bógre, The Arabidopsis protein kinase PTI1-2 is activated by convergent phosphatidic acid and oxidative stress signaling pathways downstream of PDK1 and OXI1, *J. Biol. Chem.* 281 (49) (2006) 37536–37546, <https://doi.org/10.1074/jbc.m607341200>.

- S.A. Arisz, C. Testerink, T. Munnik, Plant PA signaling via diacylglycerol kinase, *Biochim. Et. Biophys. Acta (BBA) - Mol. Cell Biol. Lipids* 1791 (9) (2009) 869–875, <https://doi.org/10.1016/j.bbaply.2009.04.006>.
- K. Audenaert, Abscisic acid determines basal susceptibility of tomato to *Botrytis cinerea* and suppresses salicylic acid-dependent signaling mechanisms, *Plant Physiol.* 128 (2002) 491–501, <https://doi.org/10.1104/pp.128.2.491>.
- A. Bah, J.D. Forman-Kay, Modulation of intrinsically disordered protein function by post-translational modifications, *J. Biol. Chem.* 291 (13) (2016) 6696–6705, <https://doi.org/10.1074/jbc.R115.695056>.
- E.P. Benito, A. ten Have, J.W. van 't Klooster, J.A.L. van Kan, Fungal and plant gene expression during synchronized infection of tomato leaves by *Botrytis cinerea*, *Eur. J. Plant Pathol.* 104 (2) (1998) 207–220, <https://doi.org/10.1023/a:1008698116106>.
- R.P. Birkenbihl, C. Diezel, I.E. Somssich, Arabidopsis WRKY33 is a key transcriptional regulator of hormonal and metabolic responses toward *Botrytis cinerea* Infection, *Plant Physiol.* 159 (1) (2012) 266–285, <https://doi.org/10.1104/pp.111.192641>.
- M. Boudsocq, M.R. Willmann, M. McCormack, H. Lee, L. Shan, P. He, J. Bush, S.-H. Cheng, J. Sheen, Differential innate immune signalling via Ca²⁺ sensor protein kinases, *Nature* 464 (7287) (2010) 418–422, <https://doi.org/10.1038/nature08794>.
- F.Y. Cao, K. Yoshioka, D. Desveaux, The roles of ABA in plant-pathogen interactions, *J. Plant Res.* 124 (4) (2011) 489–499, <https://doi.org/10.1007/s10265-011-0409-y>.
- X. Chen, L. Li, B. Xu, S. Zhao, P. Lu, Y. He, T. Ye, Y.-Q. Feng, Y. Wu, Phosphatidylinositol-specific phospholipase C2 functions in auxin-modulated root development, *Plant, Cell Environ.* 42 (5) (2019) 1441–1457, <https://doi.org/10.1111/pce.13492>.
- A. Criscuolo, S. Gribaldo, BMGE (Block Mapping and Gathering with Entropy): a new software for selection of phylogenetic informative regions from multiple sequence alignments, *BMC Evolut. Biol.* 10 (1) (2010) 210, <https://doi.org/10.1186/1471-2148-10-210>.
- G. Crooks, G. Hon, J.-M. Chandonia, S. Brenner, WebLogo: a sequence logo generator, *Genome Res.* 14 (2004) 1188–1190, <https://doi.org/10.1101/gr.849004>.
- J.M. D'Ambrosio, D. Couto, G. Fabro, D. Scuffi, L. Lamattina, T. Munnik, M.X. Andersson, M.E. Álvarez, C. Zipfel, A.M. Laxalt, Phospholipase C2 affects MAMP-triggered immunity by modulating ROS production, *Plant Physiol.* 175 (2) (2017) 970–981, <https://doi.org/10.1104/pp.17.000173>.
- C.F. de Jong, A.M. Laxalt, B.O.R. Bargmann, P.J.G.M. De Wit, M.H.A.J. Joosten, T. Munnik, Phosphatidic acid accumulation is an early response in the Cf-4/Avr4 interaction, *Plant J.* 39 (1) (2004) 1–12, <https://doi.org/10.1111/j.1365-313X.2004.02110.x>.
- M. De Torres Zabala, M.H. Bennett, W.H. Truman, M.R. Grant, Antagonism between salicylic and abscisic acid reflects early host-pathogen conflict and moulds plant defence responses, *Plant J.* 59 (3) (2009) 375–386, <https://doi.org/10.1111/j.1365-313X.2009.03875.x>.
- R. Dean, J.A.L. Van Kan, Z.A. Pretorius, K.E. Hammond-Kosack, A. Di Pietro, P.D. Spanu, J.J. Rudd, M. Dickman, R. Kahmann, J. Ellis, G.D. Foster, The Top 10 fungal pathogens in molecular plant pathology, *Mol. Plant Pathol.* 13 (4) (2012) 414–430, <https://doi.org/10.1111/j.1364-3703.2011.00783.x>.
- L.M. Di Fino, J.M. D'Ambrosio, R. Tejos, R. van Wijk, L. Lamattina, T. Munnik, G. C. Pagnussat, A.M. Laxalt, Arabidopsis phosphatidylinositol-phospholipase C2 (PLC2) is required for female gametogenesis and embryo development, *Planta* 245 (4) (2017) 717–728, <https://doi.org/10.1007/s00425-016-2634-z>.
- S.R. Eddy, Accelerated profile HMM searches, *PLOS Comput. Biol.* 7 (10) (2011) e1002195, <https://doi.org/10.1371/journal.pcbi.1002195>.
- L.-O. Essen, O. Perisic, R. Cheung, M. Katan, R.L. Williams, Crystal structure of a mammalian phosphoinositide-specific phospholipase C δ , *Nature* 380 (6575) (1996) 595–602, <https://doi.org/10.1038/380595a0>.
- P.K. Farmer, J.H. Choi, Calcium and phospholipid activation of a recombinant calcium-dependent protein kinase (DcCPK1) from carrot (*Daucus carota L.*), *Biochim. Et. Biophys. Acta (BBA) - Protein Struct. Mol. Enzymol.* 1434 (1) (1999) 6–17, [https://doi.org/10.1016/S0167-4838\(99\)00166-1](https://doi.org/10.1016/S0167-4838(99)00166-1).
- S. Ferrari, J.M. Plotnikova, G. De Lorenzo, F.M. Ausubel, Arabidopsis local resistance to *Botrytis cinerea* involves salicylic acid and camalexin and requires EDS4 and PAD2, but not SID2, EDS5 or PAD4, *Plant J.* 35 (2) (2003) 193–205, <https://doi.org/10.1046/j.1365-313X.2003.01794.x>.
- R. Galletti, C. Denoux, S. Gambetta, J. Dewdney, F.M. Ausubel, G. De Lorenzo, S. Ferrari, The AtRboHD-mediated oxidative burst elicited by oligogalacturonides in arabidopsis is dispensable for the activation of defense responses effective against *botrytis cinerea*, *Plant Physiol.* 148 (3) (2008) 1695–1706, <https://doi.org/10.1104/pp.108.127845>.
- R. Galletti, S. Ferrari, G. De Lorenzo, Arabidopsis MPK3 and MPK6 play different roles in basal and oligogalacturonide- or flagellin-induced resistance against *botrytis cinerea*, *Plant Physiol.* 157 (2) (2011) 804–814, <https://doi.org/10.1104/pp.111.174003>.
- M.H. Ghozlan, E. El-Argawy, S. Tokgöz, D.K. Lakshman, A. Mitra, Plant defense against necrotrophic pathogens, *Am. J. Plant Sci.* 11 (2020) 2122–2138, <https://doi.org/10.4236/ajps.2020.1112149>.
- G. Gonorazky, C. Guzzo, A. Laxalt, Silencing of the tomato phosphatidylinositol-phospholipase C2 (SIPLC2) reduces plant susceptibility to *Botrytis cinerea*, *Mol. Plant Pathol.* 17 (2016), <https://doi.org/10.1111/mpp.12365>.
- G. Gonorazky, L. Ramirez, A. Abd-El-Haliem, J.H. Vossen, L. Lamattina, A. ten Have, M. H.A.J. Joosten, A.M. Laxalt, The tomato phosphatidylinositol-phospholipase C2 (SIPLC2) is required for defense gene induction by the fungal elicitor xylanase, *J. Plant Physiol.* 171 (11) (2014) 959–965, <https://doi.org/10.1016/j.jplph.2014.02.008>.
- E.M. Govrin, A. Levine, The hypersensitive response facilitates plant infection by the necrotrophic pathogen *Botrytis cinerea*, *Curr. Biol.* 10 (13) (2000) 751–757, [https://doi.org/10.1016/S0960-9822\(00\)00560-1](https://doi.org/10.1016/S0960-9822(00)00560-1).
- S. Guindon, J.-F. Dufayard, V. Lefort, M. Anisimova, W. Hordijk, O. Gascuel, New algorithms and methods to estimate maximum-likelihood phylogenies: assessing the performance of PhyML 3.0, *Syst. Biol.* 59 (3) (2010) 307–321, <https://doi.org/10.1093/sysbio/syq010>.
- C. Hernández-Blanco, D. Feng, J. Hu, A. Sanchez-Vallet, L. Deslandes, F. Llorente, M. Berrocal-Lobo, H. Keller, X. Barlet, C. Sánchez-Rodríguez, L. Anderson, S. Somerville, Y. Marco, A. Molina, Impairment of cellulose synthases required for arabidopsis secondary cell wall formation enhances disease resistance, *Plant Cell* 19 (2007) 890–903, <https://doi.org/10.1105/tpc.106.048058>.
- Y. Hong, J. Zhao, L. Guo, S.C. Kim, X. Deng, G. Wang, G. Zhang, M. Li, X. Wang, Plant phospholipases D and C and their diverse functions in stress responses, *Prog. Lipid Res.* 62 (2016) 55–74.
- C.-Y. Hung, P. Aspesi Jr, M.R. Hunter, A.W. Lomax, I.Y. Perera, Phosphoinositide-signaling is one component of a robust plant defense response, *Front. Plant Sci.* 5 (2014), <https://doi.org/10.3389/fpls.2014.00267>.
- L. Hunt, L. Otterhag, J.C. Lee, T. Lasheen, J. Hunt, M. Seki, K. Shinozaki, M. Sommarin, D.J. Gilmour, C. Pical, J.E. Gray, Gene-specific expression and calcium activation of *Arabidopsis thaliana* phospholipase C isoforms, *N. Phytol.* 162 (3) (2004) 643–654, <https://doi.org/10.1111/j.1469-8137.2004.01069.x>.
- L. Iakoucheva, P. Radivojac, C. Brown, T. O'Connor, J. Sikes, Z. Obradovic, A. Dunker, The Importance of Intrinsic disorder for protein phosphorylation, *Nucleic Acids Res.* 32 (2004) 1037–1049, <https://doi.org/10.1093/nar/gkh253>.
- J. Jumper, R. Evans, A. Pritzel, T. Green, M. Figurnov, O. Ronneberger, K. Tunyasuvunakool, R. Bates, A. Žídek, A. Potapenko, A. Bridgland, C. Meyer, S.A. A. Kohl, A.J. Ballard, A. Cowie, B. Romera-Paredes, S. Nikолов, R. Jain, J. Adler, T. Back, S. Petersen, D. Reiman, E. Clancy, M. Zieliński, M. Steinegger, M. Pacholska, T. Berghammer, S. Bodenstein, D. Silver, O. Vinyals, A.W. Senior, K. Kavukcuoglu, P. Kohli, D. Hassabis, Highly accurate protein structure prediction with AlphaFold, *Nature* 596 (7873) (2021) 583–589, <https://doi.org/10.1038/s41586-021-03819-2>.
- T. Kalachova, E. Škrabálková, S. Pateyron, L. Soubigou-Taconnat, N. Djafi, S. Collin, J. Sekereš, L. Burketová, M. Potocký, P. Pejchar, E. Ruellan, DIACYLGLYCEROL KINASE 5 participates in flagellin-induced signaling in *Arabidopsis*, *Plant Physiol.* 190 (3) (2022) 1978–1996, <https://doi.org/10.1093/plphys/kiac354>.
- K. Kanehara, C.-Y. Yu, Y. Cho, W.-F. Cheong, F. Torta, G. Shui, M.R. Wenk, Y. Nakamura, *Arabidopsis AtPLC2 Is a primary phosphoinositide-specific phospholipase C in phosphoinositide metabolism and the endoplasmic reticulum stress response*, *e1005511-e1005511*, *PLOS Genet.* 11 (9) (2015), <https://doi.org/10.1371/journal.pgen.1005511>.
- M. Katan, S. Cockcroft, Phospholipase C families: Common themes and versatility in physiology and pathology, *Prog. Lipid Res.* 80 (2020) 101065, <https://doi.org/10.1016/j.plipres.2020.101065>.
- K. Katoh, D.M. Standley, MAFFT multiple sequence alignment software version 7: improvements in performance and usability, *Mol. Biol. Evol.* 30 (4) (2013) 772–780, <https://doi.org/10.1093/molbev/mst010>.
- B. Kohorn, D. Hoon, B. Minkoff, M. Sussman, S. Kohorn, Rapid oligo-galacturonide induced changes in protein phosphorylation in *Arabidopsis*, *mcp.M115.055368*, *Mol. Cell. Proteom.* 15 (2016), <https://doi.org/10.1074/mcp.M115.055368>.
- D. Laha, P. Johnen, C. Azevedo, M. Dynowski, M. Weiß, S. Capolicchio, H. Mao, T. Iven, M. Steerenberg, M. Freyer, P. Gaugler, M.K.F. de Campos, N. Zheng, I. Feussner, H. J. Jessen, S.C.M. Van Wees, A. Saïardi, G. Schaaf, VIH2 regulates the synthesis of inositol pyrophosphate InsP8 and jasmonic acid-dependent defenses in *arabidopsis*, *Plant Cell* 27 (4) (2015) 1082–1097, <https://doi.org/10.1105/tpc.114.135160>.
- C. Lamb, R.A. Dixon, The oxidative burst in plant disease resistance, *Annu. Rev. Plant Physiol. Plant Mol. Biol.* 48 (1) (1997) 251–275, <https://doi.org/10.1146/annurev.ap.48.1.251>.
- A.M. Laxalt, T. Munnik, Phospholipid signalling in plant defence, *Curr. Opin. Plant Biol.* 5 (4) (2002) 332–338, [https://doi.org/10.1016/S1369-5266\(02\)00268-6](https://doi.org/10.1016/S1369-5266(02)00268-6).
- A.M. Laxalt, N. Raho, A.T. Have, L. Lamattina, Nitric oxide is critical for inducing phosphatidic acid accumulation in xylanase-elicited tomato cells, *J. Biol. Chem.* 282 (29) (2007) 21160–21168, <https://doi.org/10.1074/jbc.m701212200>.
- S. Lee, H. Hirt, Y. Lee, Phosphatidic acid activates a wound-activated MAPK in *Glycine max*, *Plant J.* 26 (5) (2001) 479–486, <https://doi.org/10.1046/j.1365-313X.2001.01037.x>.
- F. Lemtiri-Chlieh, E.A.C. MacRobbie, C.A. Brearley, Inositol hexakisphosphate is a physiological signal regulating the K⁺-inward rectifying conductance in guard cells, *Proc. Natl. Acad. Sci.* 97 (15) (2000) 8687–8692, <https://doi.org/10.1073/pnas.140217497>.
- A. Levine, R. Tenhaken, R. Dixon, C. Lamb, H₂O₂ from the oxidative burst orchestrates the plant hypersensitive disease resistance response, *Cell* 79 (4) (1994) 583–593, [https://doi.org/10.1016/0092-8674\(94\)90544-4](https://doi.org/10.1016/0092-8674(94)90544-4).
- L. Li, Y. He, Y. Wang, S. Zhao, X. Chen, T. Ye, Y. Wu, Y. Wu, *Arabidopsis PLC2 is involved in auxin-modulated reproductive development*, *Plant J.* 84 (3) (2015) 504–515, <https://doi.org/10.1111/tpj.13016>.
- S. Liu, B. Kracher, J. Ziegler, R.P. Birkenbihl, I.E. Somssich, Negative regulation of ABA signaling by WRKY33 is critical for *Arabidopsis* immunity towards *Botrytis cinerea* 2100, *eLife* 4 (2015) e07295, <https://doi.org/10.7554/eLife.07295>.
- G. Mao, X. Meng, Y. Liu, Z. Zheng, Z. Chen, S. Zhang, Phosphorylation of a WRKY transcription factor by two pathogen-responsive MAPKs drives phytoalexin biosynthesis in *Arabidopsis*, *Plant Cell* 23 (4) (2011) 1639–1653, <https://doi.org/10.1105/tpc.111.084996>.
- D. Marino, C. Dunand, A. Puppo, N. Pauly, A burst of plant NADPH oxidases, *Trends Plant Sci.* 17 (1) (2012) 9–15, <https://doi.org/10.1016/j.tplants.2011.10.001>.
- H.J.G. Meijer, T. Munnik, Phospholipid-based signaling in plants, *Annu. Rev. Plant Biol.* 54 (1) (2003) 265–306, <https://doi.org/10.1146/annurev.aplant.54.031902.134748>.

- W. Moeder, H. Ung, S. Mosher, K. Yoshioka, SA-ABA antagonism in defense responses, *Plant Signal. Behav.* 5 (10) (2010) 1231–1233, <https://doi.org/10.4161/psb.5.10.12836>.
- J. Morales, Y. Kadota, C. Zipfel, A. Molina, M.-A. Torres, The Arabidopsis NADPH oxidases RbohD and RbohF display differential expression patterns and contributions during plant immunity, *J. Exp. Bot.* 67 (6) (2016) 1663–1676, <https://doi.org/10.1093/jxb/erv558>.
- I. Muckenschabel, B. Goodman, B. Williamson, G. Lyon, N. Deighton, Infection of leaves of *Arabidopsis thaliana* by *Botrytis cinerea*: Changes in ascorbic acid, free radicals and lipid peroxidation products, *J. Exp. Bot.* 53 (2002) 207–214, <https://doi.org/10.1093/jxb/53.367.207>.
- B. Mueller-Roeber, C. Pical, Inositol phospholipid metabolism in *Arabidopsis*. characterized and putative isoforms of inositol phospholipid kinase and phosphoinositide-specific phospholipase C, *Plant Physiol.* 130 (1) (2002) 22–46, <https://doi.org/10.1104/pp.004770>.
- T. Munnik, PI-PLC: Phosphoinositide-Phospholipase C in Plant Signaling. Phospholipases in Plant Signaling. Signaling and Communication in Plants. X. Wang. Berlin. Heidelberg, Springer, 2014, p. 20.
- T. Munnik, J.E.M. Vermeer, Osmotic stress-induced phosphoinositide and inositol phosphatase signalling in plants, *Plant, Cell Environ.* 33 (4) (2010) 655–669, <https://doi.org/10.1111/j.1365-3040.2009.02097.x>.
- P. Nicot, M. Mermier, B. Vaissière, J. Lagier, Differential spore production by *botrytis cinerea* on agar medium and plant tissue under near-ultraviolet light-absorbing polyethylene film, *Plant Dis.* 80 (1996) 555–558, <https://doi.org/10.1094/pd-80-0555>.
- T. Nuñez, A. Bottrill, A. Jones, S. Peck, Quantitative phosphoproteomic analysis of plasma membrane proteins reveals regulatory mechanisms of plant innate immune responses, *Plant J.: Cell Mol. Biol.* 51 (2007) 931–940, <https://doi.org/10.1111/j.1365-313X.2007.03192.x>.
- I.A. Pagnucco, M.V. Revuelta, H.G. Bondino, M. Brun, A. ten Have, HMMER cut-off threshold tool (HMMERCTTER): supervised classification of superfamily protein sequences with a reliable cut-off threshold, *PLOS ONE* 13 (3) (2018) e0193757, <https://doi.org/10.1371/journal.pone.0193757>.
- E. Perk, A. Arrebarrena Di Palma, S. Colman, O. Mariani, I. Cerrudo, J. D'Ambrosio, L. Robuschi, M. Pombo, H. Rosli, F. Villareal, A. Laxalt, CRISPR/Cas9-mediated phospholipase C 2 knock-out tomato plants are more resistant to *Botrytis cinerea*, *Planta* 257 (2023), <https://doi.org/10.1007/s00425-023-04147-7>.
- D. Piovesan, A. Del Conte, D. Clementel, Alexander M. Monzon, M. Bevilacqua, Maria C. Aspromonte, Javier A. Iserte, F.E. Orti, C. Marino-Buslje, Silvio C.E. Tosatto, MobiDB: 10 years of intrinsically disordered proteins, *Nucleic Acids Res.* 51 (D1) (2023) D438–D444, <https://doi.org/10.1093/nar/gkac1065>.
- I. Pokotylo, Y. Kolesnikov, V. Kravets, A. Zachowski, E. Ruelland, Plant phosphoinositide-dependent phospholipases C: Variations around a canonical theme, *Biochimie* 96 (2014) 144–157, <https://doi.org/10.1016/j.biochi.2013.07.004>.
- N. Raho, L. Ramirez, M.L. Lanteri, G. Gonorazky, L. Lamattina, A. ten Have, A.M. Laxalt, Phosphatidic acid production in chitosan-elicited tomato cells, via both phospholipase D and phospholipase C/diacylglycerol kinase, requires nitric oxide, *J. Plant Physiol.* 168 (6) (2011) 534–539, <https://doi.org/10.1016/j.jplph.2010.09.004>.
- M. Schlöffel, A. Salzer, W.-L. Wan, R. van Wijk, R. Corvo, M. Semanjski, E. Symeonidi, P. Slaby, J. Kilian, B. Macek, T. Munnik, A. Gust, The BIR2/BIR3-associated Phospholipase D gamma 1 negatively regulates plant immunity, pp.01292.02019, *Plant Physiol.* 183 (2020), <https://doi.org/10.1104/pp.19.01292>.
- L. Sheard, X. Tan, H. Mao, J. Withers, G. Ben-Nissan, T. Hinds, Y. Kobayashi, F.-F. Hsu, M. Sharon, J. Browse, S. He, J. Rizo, G. Howe, N. Zheng, Jasmonate perception by inositol phosphate-potentiated COI1-JAZ co-receptor, *Nature* 468 (2010) 400–405, <https://doi.org/10.1038/nature09430>.
- J. Szczegielniak, M. Klimecka, A. Liwosz, A. Ciesielski, S. Kaczanowski, G. Dobrowska, A. Harmon, G. Muszyńska, A WOUND-RESPONSIVE AND PHOSPHOLIPID-REGULATED MAIZE CALCIUM-DEPENDENT PROTEIN KINASE, *Plant Physiol.* 139 (2006) 1970–1983, <https://doi.org/10.1104/pp.105.066472>.
- X. Tan, L.I.A. Calderon-Villalobos, M. Sharon, C. Zheng, C.V. Robinson, M. Estelle, N. Zheng, Mechanism of auxin perception by the TIR1 ubiquitin ligase, *Nature* 446 (7136) (2007) 640–645, <https://doi.org/10.1038/nature05731>.
- C. Testerink, P.B. Larsen, D. van der Does, J.A.J. van Himbergen, T. Munnik, Phosphatidic acid binds to and inhibits the activity of *Arabidopsis* CTR1, *J. Exp. Bot.* 58 (14) (2007) 3905–3914, <https://doi.org/10.1093/jxb/erm243>.
- C. Testerink, T. Munnik, Molecular, cellular, and physiological responses to phosphatidic acid formation in plants, *J. Exp. Bot.* 62 (7) (2011) 2349–2361, <https://doi.org/10.1093/jxb/err079>.
- B. Thomma, K. Eggermont, I. Penninckx, B. Mauch-Mani, R. Vogelsang, B. Cammue, W. Broekaert, Separate jasmonate-dependent and salicylate-dependent defense-response pathways in *arabidopsis* are essential for resistance to distinct microbial pathogens, *Proc. Natl. Acad. Sci. USA* 95 (1998) 15107–15111, <https://doi.org/10.1073/pnas.95.25.15107>.
- H. Thordal-Christensen, Z. Zhang, Y. Wei, D.B. Collinge, Subcellular localization of H₂O₂ in plants. H₂O₂ accumulation in papillae and hypersensitive response during the barley—powdery mildew interaction, *Plant J.* 11 (6) (1997) 1187–1194, <https://doi.org/10.1046/j.1365-313X.1997.11061187.x>.
- M.A. Torres, ROS in biotic interactions, *Physiol. Plant.* 138 (4) (2010) 414–429, <https://doi.org/10.1111/j.1399-3054.2009.01326.x>.
- M.A. Torres, J. Dangl, J. Jones, *Arabidopsis* gp91phox homologues AtrobohD and AtrobohF are required for accumulation of reactive oxygen intermediates in the plant defense response, *Proc. Natl. Acad. Sci. USA* 99 (2002) 517–522, <https://doi.org/10.1073/pnas.012452499>.
- P. van Baarlen, E.J. Woltering, M. Staats, J.A.L. van Kan, Histochemical and genetic analysis of host and non-host interactions of *Arabidopsis* with three *Botrytis* species: an important role for cell death control, *Mol. Plant Pathol.* 8 (1) (2007) 41–54.
- A. van der Luit, T. Piatti, A. Doorn, A. Musgrave, G. Felix, T. Boller, T. Munnik, Elicitation of suspension-cultured tomato cells triggers the formation of phosphatidic acid and diacylglycerol pyrophosphate, *Plant Physiol.* 123 (2000) 1507–1516.
- J. van Kan, Licensed to kill: the lifestyle of a necrotrophic plant pathogen, *Trends Plant Sci.* 11 (2006) 247–253, <https://doi.org/10.1016/j.tplants.2006.03.005>.
- R. van Wijk, Q. Zhang, X. Zarza, M. Lamers, F.R. Marquez, A. Guardia, D. Scuffi, C. García-Mata, W. Ligterink, M.A. Haring, A.M. Laxalt, T. Munnik, Role for *Arabidopsis* PLC7 in stomatal movement, seed mucilage attachment, and leaf serration, 1721–1721, *Front. Plant Sci.* 9 (2018), <https://doi.org/10.3389/fpls.2018.01721>.
- S.P. Williams, G.E. Gillaspay, I.Y. Perera, Biosynthesis and possible functions of inositol pyrophosphates in plants, *Front. Plant Sci.* 6 (2015), <https://doi.org/10.3389/fpls.2015.00067>.
- O. Windram, P. Madhou, S. McHattie, C. Hill, R. Hickman, E. Cooke, D.J. Jenkins, C. A. Penfold, L. Baxter, E. Breeze, S.J. Kiddle, J. Rhodes, S. Atwell, D.J. Kliebenstein, Y. S. Kim, O. Stegle, K. Borgwardt, C. Zhang, A. Tabrett, R. Legaie, J. Moore, B. Finkenstadt, D.L. Wild, A. Mead, D. Rand, J. Beynon, S. Ott, V. Buchanan-Wollaston, K.J. Denby, *Arabidopsis* defense against *Botrytis cinerea*: chronology and regulation deciphered by high-resolution temporal transcriptomic analysis, *Plant Cell* 24 (9) (2012) 3530–3557.
- O. Windram, C. Stoker, K. Denby, Overview of plant defence systems: lessons from *Arabidopsis*-*Botrytis cinerea* systems biology, in: S. Fillinger, Y. Elad (Eds.), *Botrytis - the Fungus, the Pathogen and its Management in Agricultural Systems*, Springer, Cham, 2016.
- J. Xing, X. Li, X. Wang, X. Lv, L. Wang, L. Zhang, Y. Zhu, Q. Shen, F. Baluška, J. Šamaj, J. Lin, Secretion of phospholipase DΔ functions as a regulatory mechanism in plant innate immunity, *Plant Cell* 31 (12) (2019) 3015–3032, <https://doi.org/10.1105/tpc.19.00534>.
- H.-Y. Yao, H.-W. Xue, Phosphatidic acid plays key roles regulating plant development and stress responses, *J. Integr. Plant Biol.* 60 (9) (2018) 851–863, <https://doi.org/10.1111/jipb.12655>.
- Y. Zhang, H. Zhu, Q. Zhang, M. Li, M. Yan, R. Wang, L. Wang, R. Welti, W. Zhang, X. Wang, Phospholipase D 1 and phosphatidic acid regulate NADPH oxidase activity and production of reactive oxygen species in ABA-mediated stomatal closure in *Arabidopsis*, *Plant Cell* 21 (2009) 2357–2377, <https://doi.org/10.1105/tpc.108.062992>.
- J. Zhao, S. Pattada, C. Wang, M. Li, R. Welti, X. Wang, *Arabidopsis* phospholipase Dβ1 modulates defense responses to bacterial and fungal pathogens, *N. Phytol.* 199 (2013), <https://doi.org/10.1111/nph.12256>.
- Z. Zheng, S. AbuQamar, Z. Chen, T. Mengiste, *Arabidopsis* WRKY33 transcription factor is required for resistance to necrotrophic fungal pathogens, *Plant J.: Cell Mol. Biol.* 48 (2006) 592–605, <https://doi.org/10.1111/j.1365-313X.2006.02901.x>.

Supplementary Materials

Title

Arabidopsis thaliana phosphoinositide-specific phospholipase C 2 is required for *Botrytis cinerea* proliferation

Authorlist

Luciana Robuschi, Enzo A. Perk, Oriana Mariani, Ignacio Cerrudo, Fernando Villarreal, Ana M. Laxalt

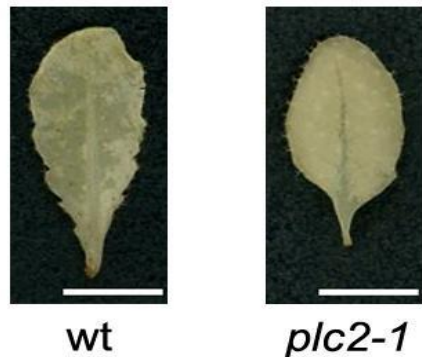


Fig. S1. Pictures of representative DAB-stained leaves after mock treatment. Leaves of four to five-week-old wild-type (wt) or *plc2-1* mutant *Arabidopsis thaliana* plants were harvested 24h after mock treatment and H₂O₂ production was detected by 3,3-diaminobenzidine (DAB) staining immediately after harvesting. (Scale bars: 0.5cm)

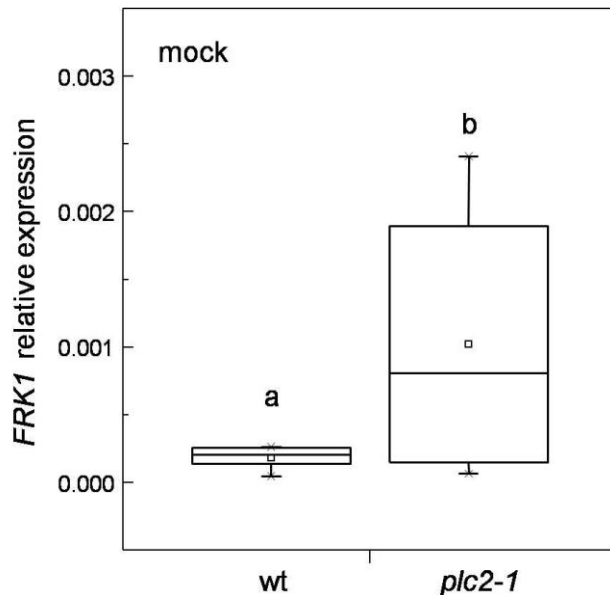


Fig. S2. Basal transcript levels of *FRK1* defense gene marker. Leaves of four to five-week-old wild-type (wt) or *plc2-1* mutant *A. thaliana* plants were harvested 24h after mock treatment. Total RNA was isolated and transcript levels of flagellin-induced receptor-like *FRK1* were determined by RT-qPCR. Transcript levels were normalized to *AtACT2*. Error bars represent standard error of three independent experiments. Different letters denote medians significantly different according to a Dunnett' test ($P < 0.05$).

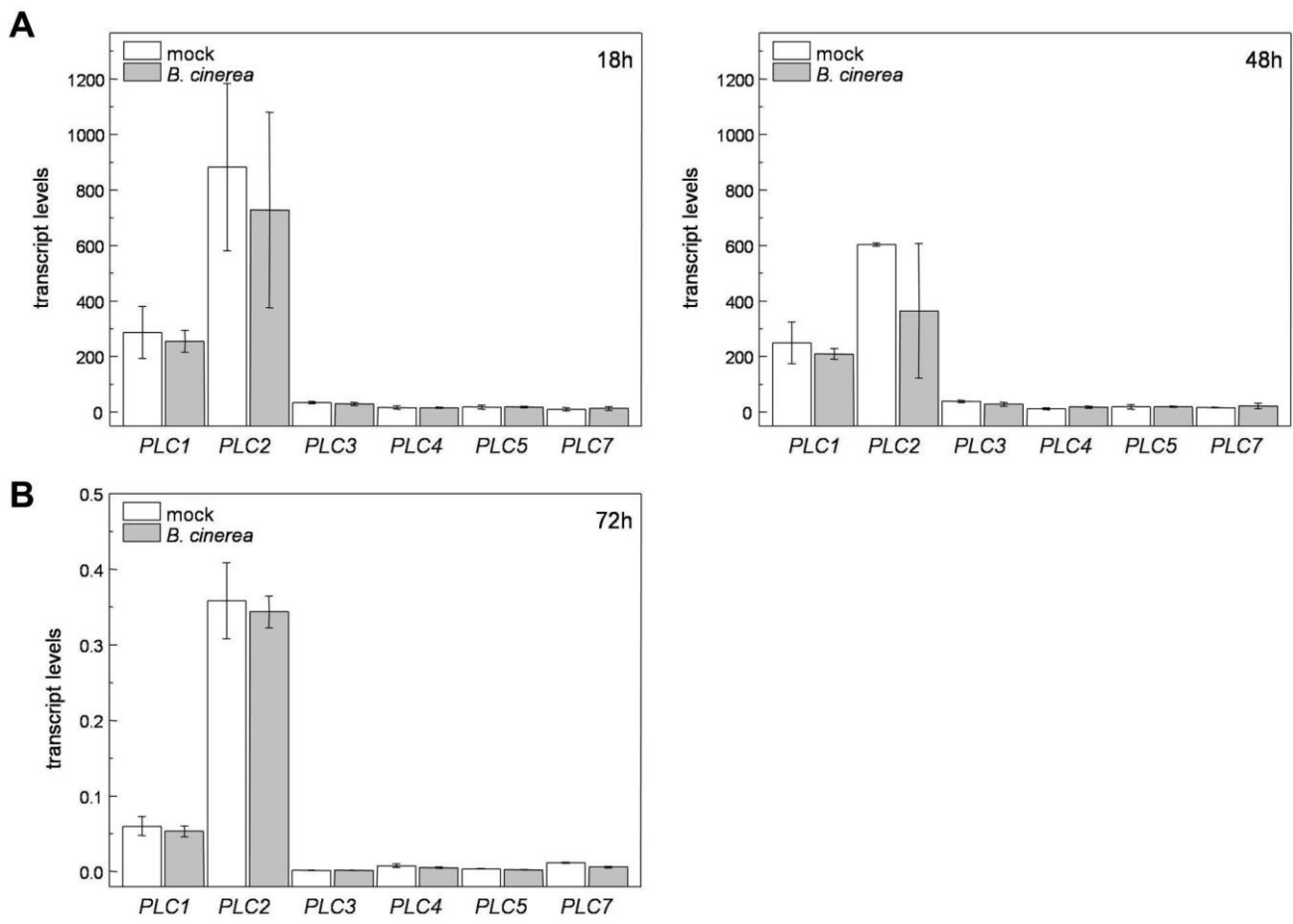


Fig. S3. Transcript levels of *AtPLC* gene family in response to *Botrytis cinerea* infection. **(A)** Leaves of four-week-old wild-type *A. thaliana* plants of Columbia-0 ecotype were drop-inoculated (5 μ l drops) with *B. cinerea* culture (5×10^5 conidia/ml) or mock inoculum. Plants were grown under 12h-light/12h-dark photoperiod. Plant material was analyzed 18 and 48 hpi. All measurements were taken in triplicates, the average of which is shown. RNA was isolated and hybridized to the ATH1 GeneChip. The data were normalized by GCOS normalization, TGT 100. This study is part of the AtGenExpress project, funded by the NSF. Results generated by the Ausubel Lab. Raw data was downloaded from the Biotic Stress Botrytis cinerea eFP at bar.utoronto.ca/eplant. **(B)** Leaves of four to five-week-old wild-type plants of Columbia-0 ecotype were drop-inoculated (5 μ l drops in the 4th to 7th leaf) with *B. cinerea* spore suspension (3×10^5 conidia/ml) or mock inoculum. Plants were grown under 8h-light/16h-dark photoperiod at 22 °C. Plant material was analyzed 72 hpi. Total RNA was isolated and transcript levels were determined by RT-qPCR. Transcript levels were normalized to *AtACT2*. Error bars represent standard error of three independent experiments.

Table S1. Primer sequences used in qRT-PCR for gene analysis.

Gene (Accession Number)	Forward Primer	Reverse Primer
<i>AtPLC1</i> (At5g58670)	5'-CTCCTGATTCTACGCAAAGGTGCG-3'	5'-GTAATGGAACTCAAACCTCCTTGTC-3'
<i>AtPLC2</i> (At3g08510)	5'-GGCTTCAATATGCAGGGTA -3'	5'-GTCAAATATGTCACTATCCGAACCAC-3'
<i>AtPLC3</i> (At4g38530)	5'-TCCAGATTTCTCGTCAAGATTGGA-3'	5'-TATAGGAAACCACTGATCGACAGC-3'
<i>AtPLC4</i> (At5g58700)	5'-TGACGAGGTTCTCGCCGAA-3'	5'-TGTTTGATGGACCTGATCGCG-3'
<i>AtPLC5</i> (At5g58690)	5'-CTTTCAACATGCAGGGCTATGGAAG-3'	5'-GAGATTATTGTTCATATAAAGTCCGG-3'
<i>AtPLC7</i> (At3g55940)	5'-GGCTTCAATATGCAGGGACT-3'	5'-CGGGTCAAATACAGCGTTGG-3'
<i>AtFRK1</i> (At2g19190)	5'-ATCTTCGCTTGAGCTCTC-3'	5'-TGCAGCGCAAGGACTAGAG-3'
<i>AtPR1</i> (At2g14610)	5'-GGCACGAGGAGCGGTAGGCG-3'	5'-CACGGCGGAGACGCCAGACA-3'
<i>AtPDF1.2</i> (At5g44420)	5'-CTCTGTTCTCTTGCTGCTTTC-3'	5'-ATAGTTGCATGATCCATGTTG-3'
<i>AtWRKY33</i> (AT2G38470)	5'-AGCAAAGAGATGAAAGGGGACAA-3'	5'-GCACTACGATTCTCGCTCTCA-3'
<i>AtACT2</i> (At3g18780)	5'-GCCATCCAAGCTGTTCTCTC-3'	5'-GAAACCCTCGTAGATTGGCA-3'

Supplementary Table S2

species	taxid	code	Order	Family	Total Sequences
<i>Pistacia vera</i>	55513	pve	Sapindales	Anacardiaceae	-
<i>Sclerocarya birrea</i>	289766	sbr	Sapindales	Anacardiaceae	-
<i>Atalantia buxifolia</i>	76974	abu	Sapindales	Rutaceae	-
<i>Citrus maxima</i>	37334	cma	Sapindales	Rutaceae	-
<i>Citrus medica</i>	171251	cme	Sapindales	Rutaceae	-
<i>Citrus reticulata</i>	85571	crt	Sapindales	Rutaceae	-
<i>Citrus ichangensis</i>	2709	cic	Sapindales	Rutaceae	-
<i>Citrus sinensis</i>	2711	csi	Sapindales	Rutaceae	-
<i>Dimocarpus longan</i>	128017	dlo	Sapindales	Sapindaceae	-
<i>Corchorus capsularis</i>	210143	ccp	Malvales	Malvaceae	-
<i>Gossypium arboreum</i>	29729	gar	Malvales	Malvaceae	-
<i>Gossypium barbadense</i>	3634	gba	Malvales	Malvaceae	-
<i>Gossypium hirsutum</i>	3635	ghi	Malvales	Malvaceae	-
<i>Gossypium turneri</i>	34284	gtu	Malvales	Malvaceae	-
<i>Theobroma cacao</i>	3641	tca	Malvales	Malvaceae	-
<i>Punica granatum</i>	22663	pgr	Myrales	Lythraceae	-
<i>Eucalyptus camaldulensis</i>	34316	eca	Myrales	Myrtaceae	-
<i>Aethionema arabicum</i>	228871	aar	Brassicaceae	Brassicaceae	2
<i>Arabidopsis halleri</i>	81970	aha	Brassicaceae	Brassicaceae	1
<i>Arabidopsis lyrata</i>	59689	aly	Brassicaceae	Brassicaceae	2
<i>Arabidopsis thaliana</i>	3702	ARATH	Brassicaceae	Brassicaceae	3
<i>Arabis alpina</i>	50452	aal	Brassicaceae	Brassicaceae	2
<i>Barbarea vulgaris</i>	50459	bvl	Brassicaceae	Brassicaceae	2
<i>Boechera stricta</i>	72658	bst	Brassicaceae	Brassicaceae	2
<i>Brassica juncea</i>	3707	bju	Brassicaceae	Brassicaceae	7
<i>Brassica napus</i>	3708	EP_Bn	Brassicaceae	Brassicaceae	4
<i>Brassica nigra</i>	3710	bni	Brassicaceae	Brassicaceae	4
<i>Brassica oleracea</i>	3712	bol	Brassicaceae	Brassicaceae	3
<i>Thellungiella halophila</i>	98038	thl	Brassicaceae	Brassicaceae	1
<i>Thellungiella parvula</i>	72663	tpa	Brassicaceae	Brassicaceae	3
<i>Thellungiella salsuginea</i>	72664	tsa	Brassicaceae	Brassicaceae	2
<i>Camelina sativa</i>	90675	cst	Brassicaceae	Brassicaceae	4
<i>Capsella grandiflora</i>	264402	cgr	Brassicaceae	Brassicaceae	2
<i>Capsella rubella</i>	81985	cru	Brassicaceae	Brassicaceae	3
<i>Cardamine hirsuta</i>	50463	chi	Brassicaceae	Brassicaceae	2
<i>Eutrema salsugineum</i>	72664	esa	Brassicaceae	Brassicaceae	1
<i>Leavenworthia alabamica</i>	310722	lal	Brassicaceae	Brassicaceae	2
<i>Raphanus raphanistrum</i>	109996	rra	Brassicaceae	Brassicaceae	1
<i>Raphanus sativus</i>	3726	rsa	Brassicaceae	Brassicaceae	3
<i>Sisymbrium irio</i>	3730	sir	Brassicaceae	Brassicaceae	3
<i>Tarenaya hassleriana</i>	28532	tha	Brassicaceae	Cleomaceae	-
<i>Moringa oleifera</i>	3735	mol	Brassicaceae	Moringaceae	-
<i>Catharanthus roseus</i>	4058	cro	Gentianales	Apocynaceae	-
<i>Coffea canephora</i>	49390	ccn	Gentianales	Rubiaceae	-
<i>Handroanthus impetiginosus</i>	429701	him	Lamiales	Bignoniaceae	-
<i>Utricularia gibba</i>	13748	ugi	Lamiales	Lentibulariaceae	-
<i>Fraxinus excelsior</i>	38873	fex	Lamiales	Oleaceae	-
<i>Olea europaea</i>	4146	oeu	Lamiales	Oleaceae	-
<i>Sesamum indicum</i>	4182	sin	Lamiales	Pedaliaceae	-
<i>Antirrhinum majus</i>	4151	ama	Lamiales	Plantaginaceae	-
<i>Ipomoea nil</i>	35883	ini	Solanales	Convolvulaceae	-
<i>Ipomoea trifida</i>	35884	itr	Solanales	Convolvulaceae	-
<i>Ipomoea triloba</i>	35885	iti	Solanales	Convolvulaceae	-

Supplementary Table S2

	<i>Capsicum annuum</i>	4072	can	Solanales	Solanaceae	1	
	<i>Capsicum baccatum</i>	33114	cba	Solanales	Solanaceae	-	
	<i>Capsicum chinense</i>	80379	cch	Solanales	Solanaceae	-	
	<i>Nicotiana attenuata</i>	49451	nat	Solanales	Solanaceae	2	
	<i>Nicotiana benthamiana</i>	4100	nbe	Solanales	Solanaceae	1	
	<i>Nicotiana sylvestris</i>	4096	nsy	Solanales	Solanaceae	5	
	<i>Nicotiana tabacum</i>	4097	EP_Nt	Solanales	Solanaceae	5	
	<i>Nicotiana tomentosiformis</i>	4098	nto	Solanales	Solanaceae	4	
	<i>Petunia axillaris</i>	33119	pax	Solanales	Solanaceae	-	
	<i>Petunia integrifolia</i>	4103	pii	Solanales	Solanaceae	-	
	<i>Petunia inflata</i>	212142	pin	Solanales	Solanaceae	-	
	<i>Solanum commersonii</i>	4109	sco	Solanales	Solanaceae	1	
	<i>Solanum lycopersicum</i>	4081	Sl	Solanales	Solanaceae	2	
	<i>Solanum melongena</i>	4111	sme	Solanales	Solanaceae	-	
	<i>Solanum pennellii</i>	28526	spe	Solanales	Solanaceae	3	
	<i>Solanum pimpinellifolium</i>	4084	spi	Solanales	Solanaceae	1	
	<i>Solanum tuberosum</i>	4113	EP_St	Solanales	Solanaceae	2	
other	<i>Populus trichocarpa</i>	3694	Pt	Malpighiales	Salicaceae	2	

Supplementary Table S1. Complete proteomes used for training (grayed) and target datasets. Phytozome and SolGenomics. A list of the taxid for each species is shown. The code used to represent the proteome is indicated. Upon classification, the amount of proteins per species is shown (both to:

Supplementary Table S2

Sequences in clade				
AtPLC2	AtPLC7	SIPLC2	SIPLC3	
-	-	-	-	-
-	-	-	-	-
-	-	-	-	-
-	-	-	-	-
-	-	-	-	-
-	-	-	-	-
-	-	-	-	-
-	-	-	-	-
-	-	-	-	-
-	-	-	-	-
-	-	-	-	-
-	-	-	-	-
-	-	-	-	-
-	-	-	-	-
-	-	-	-	-
-	-	-	-	-
-	-	-	-	-
-	-	-	-	-
-	-	-	-	-
-	-	-	-	-
1	1	-	-	-
1	-	-	-	-
1	1	-	-	-
2	1	-	-	-
1	1	-	-	-
1	1	-	-	-
1	1	-	-	-
3	4	-	-	-
2	2	-	-	-
2	2	-	-	-
1	2	-	-	-
1	-	-	-	-
1	2	-	-	-
1	1	-	-	-
2	2	-	-	-
1	1	-	-	-
1	2	-	-	-
1	1	-	-	-
1	-	-	-	-
1	1	-	-	-
1	-	-	-	-
2	1	-	-	-
1	2	-	-	-
-	-	-	-	-
-	-	-	-	-
-	-	-	-	-
-	-	-	-	-
-	-	-	-	-
-	-	-	-	-
-	-	-	-	-
-	-	-	-	-
-	-	-	-	-
-	-	-	-	-
-	-	-	-	-
-	-	-	-	-

Supplementary Table S2

-	-	1	-
-	-	-	-
-	-	-	-
-	-	1	1
-	-	1	-
-	-	3	2
-	-	2	3
-	-	2	2
-	-	-	-
-	-	-	-
-	-	-	-
-	-	1	-
-	-	1	1
-	-	-	-
-	-	2	1
-	-	-	1
-	-	1	1
-	-	-	-

Proteomes were obtained from
domain sequences in each
(total and by resulting clades).

Supplementary Table S3

name in dataset

aal0006891
aar0022982
aha0001323
aly0023435
bju0017587
bju0054347
bju0054390
bni0008423
bni0018976
bol0030865
bst0009383
bvl0006260
cgr0006708
chi0010738
cru0017904
cst0005001
cst0053941

EP_At21344

EP_Bn15537

EP_Bn29122

esa0004190

lal0016450

PLCD2_ARATH

rra0007703

rsa0006256

rsa0008740

sir0016697

thl0004190

tpa0010244

tsa0008673

aal0010318

aar0025914

aly0002245

bju0012815

bju0031816

bju0048201

bju0056302

bni0032188

bni0044927

bol0000571

bol0032673

bst0023994

bvl0014917

cgr0023518

chi0021440

cru0000945

cru0000946

cst0021419

cst0022524

EP_Bn20000

EP_Bn39490

lal0009789

PLCD7_ARATH

rsa0035577

Supplementary Table S3

sir0014386
sir0040401
tpa0011898
tpa0014187
tsa0015660
can0011047

EP_Nt17551
EP_Nt21855
EP_St27149

nat0015092
nbe0005340
nsy0026462
nsy0026463
nsy0026464
nto0026783
nto0026784
sco0009804

SI01234197
spe0025236
spe0025237

EP_Nt26954
EP_Nt49583
EP_Nt60531
EP_SI16751
EP_St20355

nat0005432
nsy0015706
nsy0015707
nto0013890
nto0013891
spe0023034
spi0016895

Pt02311223
Pt02316212
tha0002378
tha0007538

Supplementary

while the second

Supplementary Table S3

name
KFK38259.1
AA_scaffold4513_144
Araha.8409s0010.1.p
AL3G19490.t1
BjuA042922
BjuB026635
BjuB026680
BniB007959-PA
BniB043623-PA
Bol023035
Bostr.22252s0217.1.p
maker-Contig697-snap-gene-0.52-mRNA-1
Cagra.2991s0038.1.p
CARHR082830.1
Carub.0003s0766.1.p
Csa19g011870.1
Csa01g009150.1
AT3G54070.1
BnaC01g39480D
BnaA05g29670D
Thhalv10020359m
LA_scaffold1848_31
At3g08510
Raphanus_raphanistrum RrC2946 7945 12867 RrC2946_p1-mRNA-1 -1 CDS 675375303 7703 frame0
Rsa1.0_00131.1_g00013.1
Rsa1.0_00213.1_g00017.1
SI_scaffold1518_52
Thhalv10020359m PACid20183684
c0005_00677
Tsa3g06970
KFK34832.1
AA_scaffold5097_21
AL5G37220.t1
BjuA014837
BjuA044269
BjuB015398
BjuB027477
BniB014550-PA
BniB030314-PA
Bol040355
Bol045439
Bostr.20505s0162.1.p
snap_masked-Contig1893-processed-gene-0.12-mRNA-1
Cagra.0925s0006.1.p
CARHR166020.1
Carub.0005s2268.1.p
Carub.0005s2268.2.p
Csa09g068070.1
Csa06g030610.1
BnaA09g35480D-1
BnaA09g35480D-1
LA_scaffold12_22
At3g55940
Rsa1.0_02630.1_g00004.1

Supplementary Table S3

SI_scaffold139_27
SI_scaffold549_51
c0006_00254
c0007_00915
Tsa5g07020
Capang06g002208
XP_016456070
XP_016462047
M1A8D1
NIATv7_g04787.t1
Nicotiana_benthamiana Niben044Scf00001600 9708 17896 NbS00001600g0012.1 1 CDS 2132318781 5310 fra
XP_009783480.1
XP_009783481.1
XP_009783482.1
XP_009586601.1
XP_009586600.1
augustus_masked_scaffold3793_abinit_gene_1_0_mRNA_1
NP_001234197
Sopen06g017590.1
Sopen06g017590.2
XP_016469166
XP_016501093
XP_016501094
Solyc05g052760
XP_006355669
NIATv7_g15602.t1
XP_009772724.1
XP_009772725.1
XP_009605158.1
XP_009605157.1
Sopen05g031280.1
SPIMP05g0173440
POPTR_008G068400
POPTR_010G188800
Tarenaya_hassleriana scaffold00013 3520828 3524094 Th2v22402 1 CDS 1138290914 2378 frame0
Tarenaya_hassleriana scaffold00002 534256 537714 Th2v03388 1 CDS 1138260126 7538 frame0

Table S2. Detailed information in final classified dataset. The first column indicates the sequence names and the second column displays the original annotated names. The final column specifies the corresponding clade to which the sequence belongs.

Supplementary Table S3

species	clade
<i>Arabis alpina</i>	AtPLC2
<i>Aethionema arabicum</i>	AtPLC2
<i>Arabidopsis halleri</i>	AtPLC2
<i>Arabidopsis lyrata</i>	AtPLC2
<i>Brassica juncea</i>	AtPLC2
<i>Brassica juncea</i>	AtPLC2
<i>Brassica juncea</i>	AtPLC2
<i>Brassica nigra</i>	AtPLC2
<i>Brassica nigra</i>	AtPLC2
<i>Brassica oleracea</i>	AtPLC2
<i>Boechera stricta</i>	AtPLC2
<i>Barbarea vulgaris</i>	AtPLC2
<i>Capsella grandiflora</i>	AtPLC2
<i>Cardamine hirsuta</i>	AtPLC2
<i>Capsella rubella</i>	AtPLC2
<i>Camelina sativa</i>	AtPLC2
<i>Camelina sativa</i>	AtPLC2
<i>Arabidopsis thaliana</i>	AtPLC2
<i>Brassica napus</i>	AtPLC2
<i>Brassica napus</i>	AtPLC2
<i>Eutrema salsugineum</i>	AtPLC2
<i>Leavenworthia alabamica</i>	AtPLC2
<i>Arabidopsis thaliana</i>	AtPLC2
<i>Raphanus raphanistrum</i>	AtPLC2
<i>Raphanus sativus</i>	AtPLC2
<i>Raphanus sativus</i>	AtPLC2
<i>Sisymbrium irio</i>	AtPLC2
<i>Thellungiella halophila</i>	AtPLC2
<i>Thellungiella parvula</i>	AtPLC2
<i>Thellungiella salsuginea</i>	AtPLC2
<i>Arabis alpina</i>	AtPLC7
<i>Aethionema arabicum</i>	AtPLC7
<i>Arabidopsis lyrata</i>	AtPLC7
<i>Brassica juncea</i>	AtPLC7
<i>Brassica nigra</i>	AtPLC7
<i>Brassica nigra</i>	AtPLC7
<i>Brassica oleracea</i>	AtPLC7
<i>Brassica oleracea</i>	AtPLC7
<i>Boechera stricta</i>	AtPLC7
<i>Barbarea vulgaris</i>	AtPLC7
<i>Capsella grandiflora</i>	AtPLC7
<i>Cardamine hirsuta</i>	AtPLC7
<i>Capsella rubella</i>	AtPLC7
<i>Capsella rubella</i>	AtPLC7
<i>Camelina sativa</i>	AtPLC7
<i>Camelina sativa</i>	AtPLC7
<i>Brassica napus</i>	AtPLC7
<i>Brassica napus</i>	AtPLC7
<i>Leavenworthia alabamica</i>	AtPLC7
<i>Arabidopsis thaliana</i>	AtPLC7
<i>Raphanus sativus</i>	AtPLC7

Supplementary Table S3

<i>Sisymbrium irio</i>	AtPLC7
<i>Sisymbrium irio</i>	AtPLC7
<i>Thellungiella parvula</i>	AtPLC7
<i>Thellungiella parvula</i>	AtPLC7
<i>Thellungiella salsuginea</i>	AtPLC7
<i>Capsicum annuum</i>	SIPLC2
<i>Nicotiana tabacum</i>	SIPLC2
<i>Nicotiana tabacum</i>	SIPLC2
<i>Solanum tuberosum</i>	SIPLC2
<i>Nicotiana attenuata</i>	SIPLC2
<i>Nicotiana benthamiana</i>	SIPLC2
<i>Nicotiana sylvestris</i>	SIPLC2
<i>Nicotiana sylvestris</i>	SIPLC2
<i>Nicotiana sylvestris</i>	SIPLC2
<i>Nicotiana tomentosiformis</i>	SIPLC2
<i>Nicotiana tomentosiformis</i>	SIPLC2
<i>Solanum commersonii</i>	SIPLC2
<i>Solanum lycopersicum</i>	SIPLC2
<i>Solanum pennellii</i>	SIPLC2
<i>Solanum pennellii</i>	SIPLC2
<i>Nicotiana tabacum</i>	SIPLC3
<i>Nicotiana tabacum</i>	SIPLC3
<i>Nicotiana tabacum</i>	SIPLC3
<i>Solanum lycopersicum</i>	SIPLC3
<i>Solanum tuberosum</i>	SIPLC3
<i>Nicotiana attenuata</i>	SIPLC3
<i>Nicotiana sylvestris</i>	SIPLC3
<i>Nicotiana sylvestris</i>	SIPLC3
<i>Nicotiana tomentosiformis</i>	SIPLC3
<i>Nicotiana tomentosiformis</i>	SIPLC3
<i>Solanum pennellii</i>	SIPLC3
<i>Solanum pimpinellifolium</i>	SIPLC3
<i>Populus trichocarpa</i>	-
<i>Populus trichocarpa</i>	-
<i>Tarenaya hassleriana</i>	-
<i>Tarenaya hassleriana</i>	-

is per our simplified renaming,

:h each sequence belongs.